Recent Advances in Mitigating Membrane Biofouling Using Carbon-based Materials

Yichao Wu[a], Yinfeng Xia[b,f], Xinxin Jing[a], Peng Cai[a], Avanthi Deshani Igalavithana[b], Chuyang Tang[c,d,e], Daniel C.W. Tsang[g,#], Yong Sik Ok[b,*],

[a]*State Key Laboratory of Agricultural Microbiology, College of Resources and Environment, Huazhong Agricultural University, Wuhan, China*

[b]*Korea Biochar Research Center, O-Jeong Eco-Resilience Institute (OJERI) & Division of Environmental Science and Ecological Engineering, Korea University, Seoul, Republic of Korea*

[c]*Department of Civil Engineering, the University of Hong Kong, Pokfulam, Hong Kong, China*

[d]*School of Chemical Engineering, University of New South Wales, Kensington, Sydney, NSW 2033, Australia*

[e]*School of Civil and Environmental Engineering, University of New South Wales, Kensington, Sydney, NSW 2033, Australia*

[f]*College of Water Conservancy & Environmental Engineering, Zhejiang University of Water Resources & Electric Power, Hangzhou, China*

[g]*Department of Civil and Environmental Engineering, The Hong Kong Polytechnic University, Hung Hom, Kowloon, Hong Kong, China*

*Corresponding Author: E-mail: yongsikok@korea.ac.kr; Tel: 82-2-3290-3044, [#]Co-corresponding Author: E-mail: dan.tsang@polyu.edu.hk

Abstract

Biofouling is the Achilles Heel of membrane processes. The accumulation of organic foulants and growth of microorganisms on the membrane surface reduce the permeability, shorten the membrane life, and increase the energy consumption. Advancements in novel carbon-based materials (CBMs) present significant opportunities in mitigating biofouling of membrane processes. This article provides a comprehensive review of the recent progress in the application of CBMs in antibiofouling membrane. It starts with a detailed summary of the different antibiofouling mechanisms of CBM-containing membrane systems. Next, developments in membrane modification using CBMs, especially carbon nanotubes and graphene family materials, are critically reviewed. Further, the antibiofouling potential of next-generation carbon-based membranes is surveyed. Finally, the current problems and future opportunities of applying CBMs for antibiofouling membranes are discussed.

Keywords: Carbon-based materials; Carbon nanotube; Graphene, Biochar; Biofilm; Biofouling

1. Introduction

Membrane technology is a promising alternative to address water scarcity, one of the most serious challenges of our time [1]. It offers many advantages over the conventional treatment techniques, such as reliable water quality, high flexibility, reduced usage of chemical additives, and relatively low energy consumption in the overall processes [2]. Their easy operation and modular nature have enabled a number of commercially successful membrane-based water/wastewater treatment processes, including membrane bioreactors (MBRs), reverse osmosis (RO), nanofiltration (NF), ultrafiltration (UF), and microfiltration (MF) [3–6]. Many emerging processes (e.g., forward osmosis and membrane distillation) also show promising niche applications (e.g., for zero liquid discharge) [7,8].

Despite their advantages, biofouling is a main obstacle hampering the widespread use of membrane technology. It is caused by waterborne microorganisms and dissolved/particulate organic substances that are retained on the surface of or inside the membrane. Biofouling not only reduces the membrane flux and compromises the permeate quality, but also results in additional energy consumption and shortens the membrane life [9–12]. Numerous strategies have been attempted to address this problem through pretreatment of feed water [13,14], improvement of process design [15], optimization of operational conditions [16,17], membrane cleaning [18,19], and development of antibiofouling membranes [20,21].

Carbon based materials (CBMs), such as biochar, carbon nanotubes (CNTs), graphene, mesoporous carbon nanoparticles, and carbon quantum dots, show great

promise in developing novel and high-performance membranes [22–25]. These CBMs have many advantageous properties, including excellent separation properties, large surface areas, high mechanical strength, unique electrical and thermal conductivity properties, and superior antibacterial properties (Table 1). Some of these novel CBMs have enabled the fabrication of membranes of improved separation properties [25]. For example, single-layer graphene shows remarkably high water permeability (several orders of magnitude higher than conventional RO membranes) by reducing the membrane thickness to a monoatomic level [26]. Graphene family materials also exhibit exceptional antibacterial and antifouling effects originating from their electrostatic repulsion properties, hydrophilicity, and capability of inducing physical or oxidative damages to cell membrane or metabolism systems [27,28,29]. In this context, the antibiofouling ability of CBMs has attracted great interest in the field of membrane technology.

There are several recent critical reviews devoted to the advances in the application of CBMs in membrane fabrication [30–32]. These reviews mainly focused on the usage of CBMs in tuning membrane structure, physiochemical, transport and separation properties. Although CBMs demonstrated remarkable antifouling capacity, there has been no comprehensive review that addresses their fouling control mechanisms and future opportunities in membrane technology. Therefore, this article aims to provide the first review to summarize the state-of-the-art research results on the applications of CBMs in mitigating membrane biofouling. A summary of different biofouling control mechanisms is provided. The recent advances in membrane modification using CBMs

and the antibiofouling properties of next-generation graphene-based membranes are surveyed. Finally, current challenges and future opportunities are highlighted.

2. Fundamentals of biofouling control using CBMs

Membrane biofouling is triggered by the synergistic effects of microbial cells and abiotic organic foulants, such as extracellular polymeric substances (EPS) and natural organic matter. Because of the unique and tunable structures and physicochemical properties of CBMs, they open a door to develop membranes with better anti-adhesion and bactericidal properties. Novel carbon-based nanocomposites have also been developed to control biofilm formation by manipulation of bacterial signaling system.

2.1 Improvement of anti-adhesion properties

Adhesion of polysaccharides, proteins, and microbial cells on a membrane surface depends on their interactions (e.g., van der Waals and electrostatic forces and acid-base interactions) with the membrane surface [33]. These interactions are affected by the physicochemical properties of the membrane surface, such as roughness, functional groups, surface charge, and hydrophobicity [34].

In general, membranes with decreased surface roughness, reduced surface charge, and higher hydrophilicity tend to experience less biofouling. CBMs can play an important role in creating anti-adhesion membranes. Incorporation of CBMs such as GO as nanofillers in polymeric membranes induces nucleation and growth of polymer, which resulted in a smoother membrane surface [35,36]. During interfacial

polymerization, GO can retard the diffusion of monomer solution into organic solvent, which reduces the ridge formation on the membrane surface [37]. For example, the mean roughness of a thin-film composite (TFC) membrane was decreased about 80% after the addition of 800 ppm GO in the monomer aqueous solution [38]. When GO was grafted on membrane surfaces, they occupied the valleys on the surface, which flattened the surface [39,40]. Although pristine CBMs, such as CNTs and graphene, are hydrophobic (Table 1), hydrophilic functional groups can be introduced to improve the compatibility between CBMs and polymers. The hydrophilic CBMs can also induce the formation of a hydrated layer, which exerts steric exclusion effects to inhibit the adsorption of organics [41].

As bacterial cells are prone to adhere on surfaces with a water contact angle of 40–70° [42], superhydrophobic membranes with a water contact angle greater than 150° exhibit effective antibiofouling properties. The superhydrophobic surface minimizes the membrane-water contact area, which largely decreases the probability of organic foulants adhering to the membrane surface [43]. Superhydrophobic surfaces can be fabricated by the deposition of multiwall CNTs (MWCNTs) [44] or by growing a network of CNTs *in situ* using chemical vapor deposition [45]. The silane-treated rGO also showed a contact angle of 157° which can be applied as superhydrophobic coating [46].

2.2 Antimicrobial effects

Many nano-size CBMs, such as CNTs and graphene, have exhibited superior

antimicrobial properties (Figure 1 & Table 1). Membranes functionalized with these CBMs similarly exhibit excellent antimicrobial effects. These antimicrobial effects can be classified according to their different mechanisms into direct physical damage, oxidative stress, and reactive oxygen species (ROS)-independent approaches.

The sharp edges and nanostructures of nano-size CBMs can pierce microbial membranes, causing direct physical damage (Figure 1C). Recent studies found that GO can extract phospholipids from the bacterial membranes onto its own surface [47]. The loss of bacterial membrane integrity results in the release of vital intracellular substances, and eventually causes microbial deactivation. The induction of oxidative stress by nano-size CBMs is another crucial antimicrobial mechanism. Some nanomaterials such as CNT, GO, and fullerene can promote the generation of ROS via the reduction of adsorbed O_2 by cellular enzymes or metabolites (Figure 1D). Photosensitizing materials such as fullerene C60 can generate ROS under ultraviolet irradiation [48]. Excessive levels of ROS lead to the oxidation of fatty acids in the cell membrane, and disrupt the membrane integrity and vital cellular processes.

Antimicrobial effects can also be induced by ROS-independent approaches. Carbon-based nanomaterials were found to hinder cell growth by disrupting vital cellular functions and metabolic processes. For example, CNTs can inhibit the pyoverdine production of *Pseudomonas aeruginosa* PAO1, which is essential to its survival under iron-limited conditions [49]. The GO sheets with a large lateral size were shown to prevent bacterial nutrient uptake when wrapped around bacterial cells [27] (Figure 1E). Moreover, the decoration of carbon nanomaterial with other bactericidal

substances, such as Ag nanoparticles, can further improve their antimicrobial activity [50].

2.3 Biofilm signaling disruption

With the tunable carbon backbone, novel carbon nanocomposites have been developed to manipulate bacterial biofilm signaling to mitigate membrane biofouling. Quorum sensing (QS) is a crucial signaling system for biofilm formation. The accumulation of QS signals upregulates the expression of biofilm formation genes and promotes the development of mature biofilms [51]. Therefore, quenching QS signals is a favorable approach to inhibit biofilm formation on the membranes. When AHL-acylase was immobilized on GO, the modified membrane was able to hydrolyze QS signals, which subsequently reduced EPS production and biofilm development [36].

2.4 Other mechanisms

CBMs also facilitate other antibiofouling mechanisms. For example, embedding conductive CBMs enables electrically assisted fouling mitigation. Through like-charge electrostatic repulsion, gram-negative bacterial cells are repelled from negatively charged membranes [52]. Moreover, the electrochemical reduction of water generates hydrogen bubbles at the membrane surface to float the foulants (Figure 2A) [53,54]. The fouled organics on membrane surface can also be decomposed by electrochemical oxidation (Figure 2B) [55,56]. To prevent foulants from clogging the water transport channel, electrophoretic pumping cationic complexes can act as molecular brushes for

membrane cleaning (Figure 2C) [57].

3. Dosing CBMs for antibiofouling

Dosing of powdered activated carbon (PAC) is a traditional method for wastewater treatment and membrane biofouling control. Due to its large adsorptive surface, activated carbon can adsorb organics and microbes from the bulk solution. When PAC was applied in membrane bioreactors as an adsorbent, the integrity of sludge granules was increased by enhanced agglomeration with PAC and less organic foulants were available in the solution [58]. Therefore, dosing of PAC is considered an indirect approach to improve the filterability of wastewater. For instance, the addition of PAC in membrane bioreactor (MBR) reduced the total fouling resistance (R_t) by 15.9% compared to that of the control group without PAC [59]. A low PAC dosage (0.75 g/L) was found to result in a better fouling resistance than a high dosage (1.5 g/L). At a low PAC dosage, the EPS in the bulk liquid and fouled on the membrane were 84.3% and 90.0% of that in the reactor with high dosage. Consequently, the MBR with a lower dosage exhibited less irreversible fouling and a higher flux recovery rate. Further study found the lower fouling propensity was caused by the higher integrity of the sludge. At a low dosage of PAC, 84.3% less polysaccharides were released when exposed to additional shear [58].

As activated carbon is an expensive and non-regenerable material, its high operational costs hinder its practical application. In recent years, biochar has emerged as a low-cost carbon-rich by-product of pyrolysis that can be designed/engineered for

multiple applications [60,61]. The π-electron rich sites and dense polar functional groups of biochar endow it with a higher affinity towards humic acid than PAC [62], which can significantly alleviate the irreversible fouling of membranes (Figure 3). It has been reported that dosing biochar in MBR can achieve fouling mitigation effects comparable to those of activated carbon [63]. In comparison, the cost of producing biochar is less than one-tenth that of activated carbon [64]. The key physicochemical properties of biochar can be controlled by altering the pyrolysis conditions. For example, biochar generated under pure nitrogen was found to have a higher adsorption capacity than biochar prepared under low oxygen condition and PAC [62]. When applied in humic acid ultrafiltration, 12.9% less flux decline and 4.1% higher rejection were achieved by biochar compared to the use of PAC. Although CBMs dosing increases the operating cost, it can be offset by the decreased cost for membrane cleaning and the application of low-cost alternatives to PAC. Moreover, CBMs dosing can be beneficial to the wastewater treatment process, which provide substrata for biofilm growth and improve the sludge settleability and dewaterability .

4. Application of CBMs in membrane modification

CBMs with different antibiofouling mechanisms can be incorporated into membranes to improve their fouling resistance. CNTs and graphene are the most widely applied CBMs in membrane fabrication. They possess excellent thermal and mechanical properties and superior antimicrobial activities, which provide a non-leaching and non-depleting alternative to metal nanoparticles. Recent advances in their

applications in membrane modification are highlighted.

4.1 Carbon nanotubes

Single-wall CNTs (SWCNTs) are graphite sheets with a hollow cylindrical structure, while multi-wall CNTs (MWCNTs) consist of multiple rolled layers. CNTs demonstrate tremendous potential in water technology thanks to their excellent electrical, mechanical, and antifouling properties. Moreover, the hydrophobic and atomically smooth interior wall facilitates nearly frictionless water flow through the CNT core [65]. Based on the orientation and location of the CNTs in membrane, CNT-containing membranes can be further classified into vertically aligned, mixed in membranes, and coated on membrane surface (Figure 4).

Vertically-aligned (VA) CNT membranes can be prepared by casting and deposition (Figure 4A) (Baek et al., 2014; Madaeni et al., 2013). Due to the fast water transport through the CNTs, the water permeability of the modified membranes was significantly enhanced (Table 2) [66]. The flow velocity through the CNT core was at least 1000 times faster than conventional no-slip flow (Kalra et al., 2003). Due to the hydrophobic properties of pristine CNTs, the surfaces of VACNT membranes become more hydrophobic and rougher [44,66]. When filtering a bacterial suspension, the number of bacteria attached on the surface of the VACNT membrane was 2 log less than that on the control membrane without VACNT, which corresponds to 15% less reduction in the permeate flux (Baek et al., 2014). By modifying the pore size and the functional groups at the ends of the CNTs, the perm selectivity of the VACNT can be

239 further improved [67]. When zwitterions were functionalized onto the ends of the CNTs,
240 strong electrostatic interactions and a stable hydration layer were generated on the
241 membrane surface, which resulted in less protein fouling and a higher recovery rate in
242 the reverse osmosis (RO) membrane (Figure 5) [67]. Moreover, a packed VACNT array
243 without a polymeric matrix can be used directly as a membrane. The densified CNT
244 wall was found to enhance water permeability by 2,366% compared with other CNT
245 membranes [68]. Both the VACNT wall and VACNT membrane exhibited good
246 antifouling potential via decreased attachment of bacteria and inhibition of biofilm
247 formation on the membrane surface [66,68]. An assessment of the cell viability of the
248 membranes revealed that their antibiofouling effects were attributed to growth
249 inhibition rather than deactivation.

250 Due to the hydrophobic properties and strong π-π interactions between CNTs,
251 pristine CNTs have a low dispersibility in solution and poor interfacial interaction with
252 polymers. When pristine CNTs are used as a membrane additive, incompatibility
253 between the CNTs and the polymer generates nanocorridors that compromise the solute
254 rejection [69]. Therefore, chemical treatment is commonly applied to introduce
255 hydrophilic moieties such as carboxyl, hydroxyl, and amino groups on the CNTs surface
256 to improve their dispersibility and compatibility (Figure 5). CNT mixed-matrix (MM)
257 membranes can then be prepared by introducing the modified CNTs into the active layer
258 or support layer of membrane via interfacial polymerization or phase inversion (Figure
259 4B). The incorporation of CNTs into either the support or active layer enhances the
260 water permeability and fouling resistance of the resulting membrane by preventing

clogging in the skin layer and substrate pores [69,70]. The addition of CNTs to the active layer provides more effective biofouling reduction, in which the degree of the total flux loss (R_t) caused by protein fouling can be reduced by 78.7% . The bacterial growth inhibition is directly correlated with the amount of CNTs in the active layer. When the weight percentage of MWCNTs in the active layer was increased from 0.02 to 1%, the *Escherichia coli* growth inhibition rate increased from 55% to 80% [71].

Inclusion of carboxyl- and amine-surface modified CNTs into a membrane enhanced surface hydrophilicity and reduced roughness, thus increasing pure water flux and improving membrane fouling resistance against proteins and polysaccharides [70,72–74]. The smooth surface of CNT MM membranes results from the increased viscosity of the casting solution, which hinders diffusion into the organic phase during dissolution [71,74]. Grafting carboxyl and hydroxyl groups onto the CNT surface also enables further functionalization with other functional groups. For example, dodecylamine and hyperbranched poly(amine-ester) groups were functionalized on carboxylated MWCNTs, which further enhanced the protein fouling resistance and hydrophilicity of the resulting membranes [41,75]. Sulfonated CNTs produce a negatively charged surface for electrostatic repulsion [76,77]. In order to further enhance the antibacterial effect, biocidal groups have been grafted onto CNTs, such as (3-chloro-2-hydroxypropyl)-(5,5-dimethylhydantoinyl-1-ylmethyl)-dimethylammonium chloride (CDDAC), which inactivated more than 90% of *E. coli* and *Staphylococcus aureus* in 24 hours [78].

CNTs can also be immobilized onto membrane surfaces by direct deposition or

283 interfacial polymerization. Coating of the membrane surface with CNTs significantly
284 promoted its antibacterial effect. After 24 h of cross-flow filtration, little biofilm was
285 formed on a CNT-coated membrane surface, and more than 99% of the bacteria in the
286 feed were inactivated [79]. Antibacterial and antifouling activities were further
287 improved by doping with AgNPs (Figure 5) [50,80]. Deposition of the CNT-AgNP
288 composites on hollow fiber membrane was found to significantly decrease R_t by 98% .
289 Due to the extraordinary electrical conductivity of CNTs, the resistivity of surface-
290 modified membranes was found to be reduced by nearly an order of magnitude [55].
291 Therefore, electro-kinetic systems can be introduced to improve the antifouling
292 performance. By combining an electric field and a negative charge, organic foulants
293 were repelled by the negatively charged surface and electrophoresis to achieve superior
294 antifouling resistance [81,82]. Moreover, microbubbles were generated by periodic
295 electrolysis, enabling *in situ* cleaning of fouled membranes [83]. By contrast, when a
296 positive charge was applied, fouling was mitigated by electro-oxidation, in which the
297 organics adsorbed on the membrane were decomposed by electrochemical reaction
298 [55,56]. The removal of organic foulants such as humic acids was found to be a function
299 of the applied potential. At +1.5V, the permeate flux and removal efficiency were about
300 1.6 and 3.0-fold higher than those of the corresponding uncharged membrane [56].
301 Electrochemical assistance also allowed a positively charged CNT membrane to
302 inactivate bacteria and even bacteriophages attached to the membrane surface
303 [52,84,85]. Under a positive applied potential, the rate of flux declined during bacterial
304 filtration was three times lower than that of the control with no applied voltage [52].

Full recovery of the initial flux was achieved after a short flushing.

4.2 Graphene family materials

Graphene is an atomically thin sheet of sp^2-bonded carbon atoms in a hexagonal arrangement. Chemically-modified graphene derivatives, such as GO and reduced graphene oxide (rGO) are referred to graphene family materials (GFMs) [26]. Due to their low-cost mass production, chemical inertness, high tensile strength, and antimicrobial properties, GFMs have generated tremendous interest in the field of membrane modification. Similar to CNTs, GFMs can be incorporated into membranes via interfacial polymerization and phase inversion. Alternatively, they can be immobilized on the membrane surface by deposition, covalent functionalization, and layer-by-layer approaches. Recent investigations have exploited the alignability of GO on membranes. In a magnetic field, GO nanosheets could be vertically aligned on the membrane surface which maximized the edge exposure and antimicrobial activities [86].

Due to the strongly hydrophobic nature of pristine graphene, GO is prepared by oxidative modification, which introduces oxygen-containing moieties such as hydroxyl, epoxy, carbonyl, and carboxyl groups [26]. These functional groups make the use of modified graphene as a membrane additive more feasible (Table 3). A TFC membrane embedded with GO exhibited an increased hydrophilicity, negative surface potential, and decreased roughness, which resulted in greater than 95% reduction in the volume of biofilm on the membrane [37,87]. These fouling mitigation properties are directly

correlated to the oxygen-containing groups. On the contrary, the use of rGO in a MM membrane showed a detrimental effect on the antifouling properties [88]. With its higher specific surface and greater amount of oxygen-containing functional groups, a GO-blended PVDF membrane demonstrated 30% higher pure water permeability than a comparable membrane containing oxidized MWCNTs [89]. The hydrophilic membrane surface also contributed to a decrease in R_t by 6% and an enhancement of flux recovery rate by up to 5-fold (Table 3). However, a high loading of GO in a membrane induced aggregation and produced flaws in the membrane [37,38]. This negative effect can be alleviated by the synergistic interactions between CNTs and GO. In such a hybrid system, CNT-bridged GO formed a 3-D architecture that prevented aggregation and strengthened the interactions between the polymer and the nanomaterials [90,91].

Anchoring of other functional groups can further enhance antifouling performance (Figure 6). For example, due to the stronger hydrogen-bonding forces and electrostatic repulsion of the sulfonic groups, the use of sulfonated GO increased the flux recovery ratio of a GO MM membrane by 18.3% [57]. Grafted antimicrobial groups such as tannic acid, Co_3O_4, and AgNPs improved the bacterial inactivation rate of GO membranes [92–94]. The loading of GO-Co_3O_4 composites was found to decrease R_t caused by sludge fouling by 20.8% and increase the flux recovery rate by 45.4%. In addition to antimicrobial activity, antibiofouling can be achieved by influencing the biofilm signaling system as discussed before. When acylase was decorated onto the surface of GO sheets, the nanohybrid membrane was capable of hydrolyzing biofilm

signaling molecules [36] (Figure 6). Consequently, although acylase had negligible effects on organic fouling mitigation, the formation of biofilm on the membrane was reduced by 83.9%.

The unique attributes of GFMs render them a promising material to tailor the surface features of membranes. GFMs are anchored onto the membrane surface by covalent bonding and layer-by-layer (LbL) assembly. After the GFMs are deployed on the membrane surface, the hydrophobic area of the basal plane of GO can cause enhanced organic adsorption, without affecting the water flux around the edges of the GO [95]. Moreover, GO functionalization can shield the carboxyl groups on the original membrane surface and maintain the volume charge density [96]. Therefore, surface coating with GO improves the antimicrobial effect without affecting the water permeability, in which 50% reduction in R_t was achieved [97–99]. Comparing the two mainstream surface coating approaches for TFC membranes, the density of GO grafted on surfaces by covalent crosslinking is higher than that of LbL membranes, which improves the surface properties and antibiofouling effects [40]. In pressure-retarded osmosis (PRO) membranes, the LbL approach enables the formation of thin films on both sides of the membrane support, which prevents irreversible fouling inside the porous support [95].

Due to the inertness of GO, the chemical resistance of GO-containing membranes is increased. The coating layer can protect RO membranes against chlorine attack by preventing the active chlorine species from diffusing toward the selective layers [100]. Such membranes showed higher durability under frequent oxidative cleaning [101].

371 The physicochemical properties of GO also facilitate its use in photocatalytic
372 antibiofouling processes. An integrated GO-TiO_2 membrane showed 51% and 74%
373 higher protein photodegradation efficiency than membranes containing TiO_2 or GO
374 alone, respectively [102]. Photocatalysis can also be utilized for *in situ* synthesis of
375 AgNPs, which provides an alternative method to regenerate the antimicrobial properties
376 of the membrane [103].
377
378 *4.3 Other CBMs*
379 Other antimicrobial carbon-based nanomaterials such as fullerene, mesoporous
380 carbon nanoparticles (MCNs), and carbon quantum dots (CQDs) have also been
381 embedded into membranes to enhance their antifouling performance. The deposition of
382 the fullerene C60 on the membrane was found to reduce bacterial attachment and inhibit
383 microbial respiration [104]. MCNs have a higher specific surface area than GO and
384 CNTs, which makes them a promising membrane filler. A membrane containing
385 carboxylated MCN exhibited an increase in hydrophilicity and surface roughness,
386 which resulted in 80% less protein adsorption and 90% less bacterial attachment [105].
387 The CQDs have emerged as a new class of carbon nanomaterials. Their antibacterial
388 effects are caused by physical damage and ROS induction [106]. When CQDs were
389 immobilized on a membrane surface via covalent linkage, the resulting membrane
390 demonstrated better antifouling and antibacterial properties than a similar GO
391 membrane [106]. After 12-h filtration of a bacterial suspension, the flux drop of the
392 CQD membrane was 24.3%, while the permeate decrease for the GO membrane was

65.7%.

Attempts have also been made to incorporate CBMs other than carbon nanomaterials for membrane fabrication. Incorporation of PAC improved the morphology and porosity of the composite microfiltration membrane, and the selectivity of the membrane also increased at a low carbon loading [107]. Blending PAC and hydrophilic PEG resulted in improved permeability, hydrophilicity, roughness, and organic fouling resistance [108]. As an alternative to PAC, biochar has also been applied in membrane modification in the latest studies. Comparable antibiofouling performance was achieved, which indicated the great potential for biochar in practical applications [109].

The membranes modified by CBMs have exhibited superior antibiofouling properties which outperform the commercial membranes. Among different modification approaches, the MM membrane can be readily realized for industrial scale production. The fabrication procedure requires to load CBMs into the active or support layer, which can be integrated into the existing production lines of polymeric membranes. The low price of CBMs like MWCNTs makes MM membrane feasible to scale up at a competitive cost. Compared with MM membrane, the processing of CBMs into the primary rejection layer, for example VA CNT membranes, is often complicated and time consuming. The incorporation of CBMs may also compromise the salt rejection capability by forming defects or decreasing crosslinking density . Moreover, the leachability of nano-size CBMs into aquatic environments or product water should be considered, especially for the surface-modified membranes. The deposited CBMs

on membrane surfaces directly interact with the feed water which are more likely to release into environments.

5. Next-generation membranes fabricated using carbon-based materials

The excellent separation properties of GFMs offer great opportunities to design novel membrane processes. Nanoporous graphene (NPG) and graphene oxide frameworks (GOFs) have been proposed as next-generation membranes for desalination. To overcome the impermeability of pristine graphene, NPG is generated by introducing nanometer pores via plasma etching or bombardment [110]. Due to its well-defined nanopores and monoatomic thickness, NPG exhibits outstanding size exclusion properties and water permeability. However, the scale-up of NPG membranes remains challenging, and the antibiofouling properties of NPG are largely unexplored. It has been recognized that rGO and graphite have been found to induce more intense oxidative stress than GO and graphite oxide [111]. Functional groups can be introduced to decorate the nanopores to mitigate fouling and prevent clogging. Therefore, NPG is expected to have good biofouling resistance properties.

GOFs, which comprise stacked GO nanosheets, are another advanced alternative to the existing desalination membranes. The GO laminates can be simply prepared by filtration or LbL deposition to produce freestanding or substrate-supported GOF membranes. Unlike membranes produced by surface modification, the stacked GO itself serves as the selective layer in GOF membranes. Water molecules are transported through the nanochannels between adjacent GO sheets, while the solute can be excluded.

To achieve the trade-off between permeability and membrane selectivity, GO-CNT composite membranes were developed in which CNTs control the interlayer space between graphene sheets . The pure water permeability was enhanced by more than 2 times, while high salt rejection ratio was maintained. The intercalation of CNT with GO can also enhance the mechanical stability of GOF membranes against cross flow . The ability of GO laminates to sustain long-term filtration of Kraft black liquor has been demonstrated [112]. The accumulation of organic foulants on GO laminates was dependent on their interlayer spacing, the hydrophilicity of the GO, and the chemical properties of the cross-linker [113]. When more GO layers were introduced, the organic fouling propensity of the membrane was reduced and its antimicrobial activity was enhanced [114]. As stacked GO tends to disperse in water, rGO nanosheets are applied to reduce the swelling of the GOF. To minimize fouling on the hydrophobic rGO surface, hydrophilic coatings can be applied via hydrophilic adhesive polydopamine (pDA) deposition [115]. Moreover, the chemistry and morphology of GO can be tuned to optimize GO laminates for different purposes [116]. For example, the hydrophobicity of GO laminates is controlled by adjusting their oxidation state via photoreduction. A negative charge can be introduced to the nanochannels via *in situ* post-treatment with free chlorine, which offers great potential to generate electrostatic repulsion [117].

Although the emerging GFMs have showed promising performance, most of these applications are limited to small-scale devices. The poor mechanical stability of GFMs under practical hydrodynamic flow condition is another major challenge in long-term application. In order to resolve these issues, recent advancements have improved the

scalability of GOF membrane via spray coating and shear alignment . The resistance to shear stress was enhanced by the additional interfacial adhesive layer between GO and support layers. With exceptional resistance to chemical cleaning, the GOF membrane can be a scalable alternative to commercial polymeric membranes in the desalination industry.

6. Conclusions and future prospects

In recent years, substantial advances have been made in the application of various CBMs for membrane antibiofouling. The use of CBMs shows great promise in addressing the problem of biofouling and revolutionizing conventional membrane processes. Dosing CBMs can effectively reduce membrane contamination by foulants from the bulk liquid. Surface modification has shown promising antibiofouling activity via tailoring the membrane surface roughness, hydrophilicity, electrostatic potential, and antimicrobial properties. Based on synergistic effects of CBMs with other nanomaterials, additional highly desirable characteristics and functionalities can be introduced. Next-generation graphene-based membranes provide ultrafast water transport and antibiofouling potential, which outperform current membrane processes. However, many challenges still limit the practical application of these novel membrane processes. In order to tackle the water crisis, further scientific and technical contributions will be vital to fully explore the potential of membrane systems.

Firstly, industrialization of these cutting-edge membrane systems is still problematic. For example, due to the synthetic complexity and difficulties in scalable

processing, large-scale production of NPG is still in its infancy [30]. The commercialization of modified membranes using CBMs is relatively easier compared to NPG and GOF [23]. Therefore, novel technologies and production techniques are required to close the gap between research and industrial utilization. The application of sustainable and cost-effective CBMs such as biochar is one alternative to promote system sustainability and reduce production cost.

Secondly, the long-term durability and antifouling performance of these membranes should be further evaluated. Over a long period of operation, microbes can condition the membrane surface by EPS and dead cell components that facilitate subsequent adhesion of microbes and eventually cause severe biofouling. Therefore, more resources need to be invested to provide a comprehensive understanding of long-term antibiofouling activity of next-generation membranes, whose superior rejection and water permeability properties do not necessarily translate into long-term antibiofouling activity.

Finally, appropriate antibiofouling characterization approaches should be adopted. Measurement of the number of colony forming units (CFUs) is the mainstream method to evaluate the antimicrobial effect of a membrane. However, these results can be misleading due to cell aggregation under stress conditions [118]. Moreover, nondestructive and real-time approaches should be applied to monitor the biofouling processes of membrane. The most widely applied technique is to stain the bacteria attached on the membrane after disassembly of the membrane module and observe them under a confocal microscope. However, the resultant observation provides only a

snapshot of the fouling process, and artificial effects are induced during the examination. To address this issue, nondestructive methods to assess biofouling have been developed using optical coherence tomography and confocal microscope compatible microfluidics [119,120].

Acknowledgements

We thank Professor Yuan Chen, the University of Sydney, for his helpful comments on the manuscript. This work was supported by the National Natural Science Foundation of China (41807024, 41877029), the National Basic Research Program of China (2016YFD0800206) and the Fundamental Research Funds for the Central Universities (Program No. 52902-0900201674).

References

[1] M.A. Shannon, P.W. Bohn, M. Elimelech, J.G. Georgiadis, B.J. Mariñas, A.M. Mayes, Science and technology for water purification in the coming decades, Nature. 452 (2008) 301–310. doi:10.1038/nature06599.

[2] G. Kang, Y. Cao, Development of antifouling reverse osmosis membranes for water treatment: A review, Water Res. 46 (2012) 584–600. doi:10.1016/J.WATRES.2011.11.041.

[3] M. Elimelech, W.A. Phillip, The Future of Seawater Desalination: Energy, Technology, and the Environment, Science (80-.). 333 (2011) 712–717. doi:10.1126/science.1200488.

525 [4] M.M. Pendergast, E.M.V. Hoek, A review of water treatment membrane
526 nanotechnologies, Energy Environ. Sci. 4 (2011) 1946.
527 doi:10.1039/c0ee00541j.
528 [5] K.P. Lee, T.C. Arnot, D. Mattia, A review of reverse osmosis membrane
529 materials for desalination—Development to date and future potential, J. Memb.
530 Sci. 370 (2011) 1–22. doi:10.1016/J.MEMSCI.2010.12.036.
531 [6] W. Yang, N. Cicek, J. Ilg, State-of-the-art of membrane bioreactors:
532 Worldwide research and commercial applications in North America, J. Memb.
533 Sci. 270 (2006) 201–211. doi:10.1016/J.MEMSCI.2005.07.010.
534 [7] E.W. Tow, D.M. Warsinger, A.M. Trueworthy, J. Swaminathan, G.P. Thiel,
535 S.M. Zubair, A.S. Myerson, J.H. Lienhard V, Comparison of fouling
536 propensity between reverse osmosis, forward osmosis, and membrane
537 distillation, J. Memb. Sci. 556 (2018) 352–364.
538 doi:10.1016/J.MEMSCI.2018.03.065.
539 [8] T.Y. Cath, A.E. Childress, M. Elimelech, Forward osmosis: Principles,
540 applications, and recent developments, J. Memb. Sci. 281 (2006) 70–87.
541 doi:10.1016/J.MEMSCI.2006.05.048.
542 [9] V. Kochkodan, N. Hilal, A comprehensive review on surface modified polymer
543 membranes for biofouling mitigation, Desalination. 356 (2015) 187–207.
544 doi:10.1016/J.DESAL.2014.09.015.
545 [10] S.E. Kwan, E. Bar-Zeev, M. Elimelech, Biofouling in forward osmosis and
546 reverse osmosis: Measurements and mechanisms, J. Memb. Sci. 493 (2015)

703–708. doi:10.1016/J.MEMSCI.2015.07.027.

[11] Q. She, R. Wang, A.G. Fane, C.Y. Tang, Membrane fouling in osmotically driven membrane processes: A review, J. Memb. Sci. 499 (2016) 201–233. doi:10.1016/J.MEMSCI.2015.10.040.

[12] M. Xie, J. Lee, L.D. Nghiem, M. Elimelech, Role of pressure in organic fouling in forward osmosis and reverse osmosis, J. Memb. Sci. 493 (2015) 748–754. doi:10.1016/J.MEMSCI.2015.07.033.

[13] A. Maartens, P. Swart, E.P. Jacobs, Feed-water pretreatment: methods to reduce membrane fouling by natural organic matter, J. Memb. Sci. 163 (1999) 51–62. doi:10.1016/S0376-7388(99)00155-6.

[14] T. Carroll, S. King, S.. Gray, B.. Bolto, N.. Booker, The fouling of microfiltration membranes by NOM after coagulation treatment, Water Res. 34 (2000) 2861–2868. doi:10.1016/S0043-1354(00)00051-8.

[15] M. Stoller, B. De Caprariis, A. Cicci, N. Verdone, M. Bravi, A. Chianese, About proper membrane process design affected by fouling by means of the analysis of measured threshold flux data, Sep. Purif. Technol. 114 (2013) 83–89. doi:10.1016/J.SEPPUR.2013.04.041.

[16] Z. Beril Gönder, S. Arayici, H. Barlas, Advanced treatment of pulp and paper mill wastewater by nanofiltration process: Effects of operating conditions on membrane fouling, Sep. Purif. Technol. 76 (2011) 292–302. doi:10.1016/J.SEPPUR.2010.10.018.

[17] Z. Huang, S.L. Ong, H.Y. Ng, Submerged anaerobic membrane bioreactor for

low-strength wastewater treatment: Effect of HRT and SRT on treatment performance and membrane fouling, Water Res. 45 (2011) 705–713. doi:10.1016/J.WATRES.2010.08.035.

[18] A. Al-Amoudi, R.W. Lovitt, Fouling strategies and the cleaning system of NF membranes and factors affecting cleaning efficiency, J. Memb. Sci. 303 (2007) 4–28. doi:10.1016/J.MEMSCI.2007.06.002.

[19] J.P. Chen, S.. Kim, Y.. Ting, Optimization of membrane physical and chemical cleaning by a statistically designed approach, J. Memb. Sci. 219 (2003) 27–45. doi:10.1016/S0376-7388(03)00174-1.

[20] C.X. Liu, D.R. Zhang, Y. He, X.S. Zhao, R. Bai, Modification of membrane surface for anti-biofouling performance: Effect of anti-adhesion and anti-bacteria approaches, J. Memb. Sci. 346 (2010) 121–130. doi:10.1016/J.MEMSCI.2009.09.028.

[21] L. Liu, F. Zhao, J. Liu, F. Yang, Preparation of highly conductive cathodic membrane with graphene (oxide)/PPy and the membrane antifouling property in filtrating yeast suspensions in EMBR, J. Memb. Sci. 437 (2013) 99–107. doi:10.1016/J.MEMSCI.2013.02.045.

[22] A. Bianco, Y. Chen, Y. Chen, D. Ghoshal, R.H. Hurt, Y.A. Kim, N. Koratkar, V. Meunier, M. Terrones, A carbon science perspective in 2018: Current achievements and future challenges, Carbon N. Y. 132 (2018) 785–801. doi:10.1016/J.CARBON.2018.02.058.

[23] Z. Yang, X.-H. Ma, C.Y. Tang, Recent development of novel membranes for

desalination, Desalination. 434 (2018) 37–59. doi:10.1016/J.DESAL.2017.11.046.

[24] C.Y. Tang, Z. Yang, H. Guo, J.J. Wen, L.D. Nghiem, E. Cornelissen, Potable Water Reuse through Advanced Membrane Technology, Environ. Sci. Technol. 52 (2018) 10215–10223. doi:10.1021/acs.est.8b00562.

[25] M.S. Mauter, M. Elimelech, Environmental Applications of Carbon-Based Nanomaterials, Environ. Sci. Technol. 42 (2008) 5843–5859. doi:10.1021/es8006904.

[26] A. Bianco, H.-M. Cheng, T. Enoki, Y. Gogotsi, R.H. Hurt, N. Koratkar, T. Kyotani, M. Monthioux, C.R. Park, J.M.D. Tascon, J. Zhang, All in the graphene family – A recommended nomenclature for two-dimensional carbon materials, Carbon N. Y. 65 (2013) 1–6. doi:10.1016/J.CARBON.2013.08.038.

[27] H.M. Hegab, A. ElMekawy, L. Zou, D. Mulcahy, C.P. Saint, M. Ginic-Markovic, The controversial antibacterial activity of graphene-based materials, Carbon N. Y. 105 (2016) 362–376. doi:10.1016/J.CARBON.2016.04.046.

[28] G.F. Schneider, Q. Xu, S. Hage, S. Luik, J.N.H. Spoor, S. Malladi, H. Zandbergen, C. Dekker, Tailoring the hydrophobicity of graphene for its use as nanopores for DNA translocation, Nat. Commun. 4 (2013) 2619. doi:10.1038/ncomms3619.

[29] R. Das, C.D. Vecitis, A. Schulze, B. Cao, A.F. Ismail, X. Lu, J. Chen, S. Ramakrishna, Recent advances in nanomaterials for water protection and monitoring, Chem. Soc. Rev. 46 (2017) 6946–7020.

613 doi:10.1039/C6CS00921B.
614 [30] S. Dervin, D.D. Dionysiou, S.C. Pillai, 2D nanostructures for water
615 purification: graphene and beyond, Nanoscale. 8 (2016) 15115–15131.
616 doi:10.1039/C6NR04508A.
617 [31] K. Goh, H.E. Karahan, L. Wei, T.-H. Bae, A.G. Fane, R. Wang, Y. Chen,
618 Carbon nanomaterials for advancing separation membranes: A strategic
619 perspective, Carbon N. Y. 109 (2016) 694–710.
620 doi:10.1016/J.CARBON.2016.08.077.
621 [32] M. Sianipar, S.H. Kim, K. Khoiruddin, F. Iskandar, I.G. Wenten,
622 Functionalized carbon nanotube (CNT) membrane: progress and challenges,
623 RSC Adv. 7 (2017) 51175–51198. doi:10.1039/C7RA08570B.
624 [33] C.Y. Tang, T.H. Chong, A.G. Fane, Colloidal interactions and fouling of NF
625 and RO membranes: A review, Adv. Colloid Interface Sci. 164 (2011) 126–
626 143. doi:10.1016/J.CIS.2010.10.007.
627 [34] E.M. V. Hoek, S. Bhattacharjee, M. Elimelech, Effect of Membrane Surface
628 Roughness on Colloid−Membrane DLVO Interactions, (2003).
629 doi:10.1021/LA027083C.
630 [35] Z. Zhu, J. Jiang, X. Wang, X. Huo, Y. Xu, Q. Li, L. Wang, Improving the
631 hydrophilic and antifouling properties of polyvinylidene fluoride membrane by
632 incorporation of novel nanohybrid GO@SiO2 particles, Chem. Eng. J. 314
633 (2017) 266–276. doi:10.1016/j.cej.2016.12.038.
634 [36] Z. Zhu, L. Wang, Q. Li, A bioactive poly (vinylidene fluoride)/graphene

635 oxide@acylase nanohybrid membrane: Enhanced anti-biofouling based on
636 quorum quenching, J. Memb. Sci. 547 (2018) 110–122.
637 doi:10.1016/J.MEMSCI.2017.10.041.
638 [37] H.-R. Chae, C.-H. Lee, P.-K. Park, I.-C. Kim, J.-H. Kim, Synergetic effect of
639 graphene oxide nanosheets embedded in the active and support layers on the
640 performance of thin-film composite membranes, J. Memb. Sci. 525 (2017) 99–
641 106. doi:10.1016/J.MEMSCI.2016.10.034.
642 [38] L. Shen, S. Xiong, Y. Wang, Graphene oxide incorporated thin-film composite
643 membranes for forward osmosis applications, Chem. Eng. Sci. 143 (2016) 194–
644 205. doi:10.1016/J.CES.2015.12.029.
645 [39] A. Soroush, W. Ma, Y. Silvino, M.S. Rahaman, Surface modification of thin
646 film composite forward osmosis membrane by silver-decorated graphene-oxide
647 nanosheets, Environ. Sci. Nano. 2 (2015) 395–405. doi:10.1039/C5EN00086F.
648 [40] H.M. Hegab, A. ElMekawy, T.G. Barclay, A. Michelmore, L. Zou, C.P. Saint,
649 M. Ginic-Markovic, Fine-Tuning the Surface of Forward Osmosis Membranes
650 via Grafting Graphene Oxide: Performance Patterns and Biofouling Propensity,
651 ACS Appl. Mater. Interfaces. 7 (2015) 18004–18016.
652 doi:10.1021/acsami.5b04818.
653 [41] X. Zhao, J. Ma, Z. Wang, G. Wen, J. Jiang, F. Shi, L. Sheng, Hyperbranched-
654 polymer functionalized multi-walled carbon nanotubes for poly (vinylidene
655 fluoride) membranes: From dispersion to blended fouling-control membrane,
656 Desalination. 303 (2012) 29–38. doi:10.1016/J.DESAL.2012.07.009.

[42] Y. Arima, H. Iwata, Effect of wettability and surface functional groups on protein adsorption and cell adhesion using well-defined mixed self-assembled monolayers, Biomaterials. 28 (2007) 3074–3082. doi:10.1016/j.biomaterials.2007.03.013.

[43] A. Marmur, Super-hydrophobicity fundamentals: implications to biofouling prevention, Biofouling. 22 (2006) 107–115. doi:10.1080/08927010600562328.

[44] S.S. Madaeni, S. Zinadini, V. Vatanpour, Preparation of superhydrophobic nanofiltration membrane by embedding multiwalled carbon nanotube and polydimethylsiloxane in pores of microfiltration membrane, Sep. Purif. Technol. 111 (2013) 98–107. doi:10.1016/J.SEPPUR.2013.03.033.

[45] Y. Dong, L. Ma, C.Y. Tang, F. Yang, X. Quan, D. Jassby, M.J. Zaworotko, M.D. Guiver, Stable Superhydrophobic Ceramic-Based Carbon Nanotube Composite Desalination Membranes, Nano Lett. 18 (2018) 5514–5521. doi:10.1021/acs.nanolett.8b01907.

[46] J. Lee, H.-R. Chae, Y.J. Won, K. Lee, C.-H. Lee, H.H. Lee, I.-C. Kim, J. Lee, Graphene oxide nanoplatelets composite membrane with hydrophilic and antifouling properties for wastewater treatment, J. Memb. Sci. 448 (2013) 223–230. doi:10.1016/J.MEMSCI.2013.08.017.

[47] Y. Tu, M. Lv, P. Xiu, T. Huynh, M. Zhang, M. Castelli, Z. Liu, Q. Huang, C. Fan, H. Fang, R. Zhou, Destructive extraction of phospholipids from Escherichia coli membranes by graphene nanosheets, Nat. Nanotechnol. 8 (2013) 594–601. doi:10.1038/nnano.2013.125.

[48] S.-R. Chae, E.M. Hotze, M.R. Wiesner, Evaluation of the Oxidation of Organic Compounds by Aqueous Suspensions of Photosensitized Hydroxylated-C_{60} Fullerene Aggregates, Environ. Sci. Technol. 43 (2009) 6208–6213. doi:10.1021/es901165q.

[49] A. Mohanty, L. Wei, L. Lu, Y. Chen, B. Cao, Impact of Sublethal Levels of Single-Wall Carbon Nanotubes on Pyoverdine Production in *Pseudomonas aeruginosa* and Its Environmental Implications, Environ. Sci. Technol. Lett. 2 (2015) 105–111. doi:10.1021/acs.estlett.5b00057.

[50] A. Yoosefi Booshehri, R. Wang, R. Xu, The effect of re-generable silver nanoparticles/multi-walled carbon nanotubes coating on the antibacterial performance of hollow fiber membrane, Chem. Eng. J. 230 (2013) 251–259. doi:10.1016/J.CEJ.2013.06.068.

[51] M.B. Miller, B.L. Bassler, Quorum Sensing in Bacteria, Annu. Rev. Microbiol. 55 (2001) 165–199. doi:10.1146/annurev.micro.55.1.165.

[52] C.-F. de Lannoy, D. Jassby, K. Gloe, A.D. Gordon, M.R. Wiesner, Aquatic Biofouling Prevention by Electrically Charged Nanocomposite Polymer Thin Film Membranes, Environ. Sci. Technol. 47 (2013) 2760–2768. doi:10.1021/es3045168.

[53] B.S. Lalia, F.E. Ahmed, T. Shah, N. Hilal, R. Hashaikeh, Electrically conductive membranes based on carbon nanostructures for self-cleaning of biofouling, Desalination. 360 (2015) 8–12. doi:10.1016/J.DESAL.2015.01.006.

[54] X. Sun, J. Wu, Z. Chen, X. Su, B.J. Hinds, Fouling Characteristics and

Electrochemical Recovery of Carbon Nanotube Membranes, Adv. Funct. Mater. 23 (2013) 1500–1506. doi:10.1002/adfm.201201265.

[55] W. Duan, A. Ronen, S. Walker, D. Jassby, Polyaniline-Coated Carbon Nanotube Ultrafiltration Membranes: Enhanced Anodic Stability for *In Situ* Cleaning and Electro-Oxidation Processes, ACS Appl. Mater. Interfaces. 8 (2016) 22574–22584. doi:10.1021/acsami.6b07196.

[56] X. Fan, H. Zhao, Y. Liu, X. Quan, H. Yu, S. Chen, Enhanced Permeability, Selectivity, and Antifouling Ability of CNTs/Al_2O_3 Membrane under Electrochemical Assistance, Environ. Sci. Technol. 49 (2015) 2293–2300. doi:10.1021/es5039479.

[57] S. Ayyaru, Y.-H. Ahn, Application of sulfonic acid group functionalized graphene oxide to improve hydrophilicity, permeability, and antifouling of PVDF nanocomposite ultrafiltration membranes, J. Memb. Sci. 525 (2017) 210–219. doi:10.1016/J.MEMSCI.2016.10.048.

[58] M. Remy, V. Potier, H. Temmink, W. Rulkens, Why low powdered activated carbon addition reduces membrane fouling in MBRs, Water Res. 44 (2010) 861–867. doi:10.1016/J.WATRES.2009.09.046.

[59] Z. Ying, G. Ping, Effect of powdered activated carbon dosage on retarding membrane fouling in MBR, Sep. Purif. Technol. 52 (2006) 154–160. doi:10.1016/J.SEPPUR.2006.04.010.

[60] M. Ahmad, A.U. Rajapaksha, J.E. Lim, M. Zhang, N. Bolan, D. Mohan, M. Vithanage, S.S. Lee, Y.S. Ok, Biochar as a sorbent for contaminant

723 management in soil and water: A review, Chemosphere. 99 (2014) 19–33.
724 doi:10.1016/j.chemosphere.2013.10.071.
725 [61] A.U. Rajapaksha, S.S. Chen, D.C.W. Tsang, M. Zhang, M. Vithanage, S.
726 Mandal, B. Gao, N.S. Bolan, Y.S. Ok, Engineered/designer biochar for
727 contaminant removal/immobilization from soil and water: Potential and
728 implication of biochar modification, Chemosphere. 148 (2016) 276–291.
729 doi:10.1016/j.chemosphere.2016.01.043.
730 [62] K.H. Chu, V. Shankar, C.M. Park, J. Sohn, A. Jang, Y. Yoon, Evaluation of
731 fouling mechanisms for humic acid molecules in an activated biochar-
732 ultrafiltration hybrid system, Chem. Eng. J. 326 (2017) 240–248.
733 doi:10.1016/J.CEJ.2017.05.161.
734 [63] X.-F. Sima, Y.-Y. Wang, X.-C. Shen, X.-R. Jing, L.-J. Tian, H.-Q. Yu, H.
735 Jiang, Robust biochar-assisted alleviation of membrane fouling in MBRs by
736 indirect mechanism, Sep. Purif. Technol. 184 (2017) 195–204.
737 doi:10.1016/J.SEPPUR.2017.04.046.
738 [64] C. Luo, F. Lü, L. Shao, P. He, Application of eco-compatible biochar in
739 anaerobic digestion to relieve acid stress and promote the selective colonization
740 of functional microbes, Water Res. 68 (2015) 710–718.
741 doi:10.1016/J.WATRES.2014.10.052.
742 [65] B.J. Hinds, N. Chopra, T. Rantell, R. Andrews, V. Gavalas, L.G. Bachas,
743 Aligned Multiwalled Carbon Nanotube Membranes, Science (80-.). 303 (2004)
744 62–65. doi:10.1126/science.1092048.

[66] Y. Baek, C. Kim, D.K. Seo, T. Kim, J.S. Lee, Y.H. Kim, K.H. Ahn, S.S. Bae, S.C. Lee, J. Lim, K. Lee, J. Yoon, High performance and antifouling vertically aligned carbon nanotube membrane for water purification, J. Memb. Sci. 460 (2014) 171–177. doi:10.1016/J.MEMSCI.2014.02.042.

[67] W.-F. Chan, E. Marand, S.M. Martin, Novel zwitterion functionalized carbon nanotube nanocomposite membranes for improved RO performance and surface anti-biofouling resistance, J. Memb. Sci. 509 (2016) 125–137. doi:10.1016/J.MEMSCI.2016.02.014.

[68] B. Lee, Y. Baek, M. Lee, D.H. Jeong, H.H. Lee, J. Yoon, Y.H. Kim, A carbon nanotube wall membrane for water treatment, Nat. Commun. 6 (2015) 7109. doi:10.1038/ncomms8109.

[69] X. Song, L. Wang, L. Mao, Z. Wang, Nanocomposite Membrane with Different Carbon Nanotubes Location for Nanofiltration and Forward Osmosis Applications, ACS Sustain. Chem. Eng. 4 (2016) 2990–2997. doi:10.1021/acssuschemeng.5b01575.

[70] M. Son, H. Choi, L. Liu, E. Celik, H. Park, H. Choi, Efficacy of carbon nanotube positioning in the polyethersulfone support layer on the performance of thin-film composite membrane for desalination, Chem. Eng. J. 266 (2015) 376–384. doi:10.1016/J.CEJ.2014.12.108.

[71] W. Falath, A. Sabir, K.I. Jacob, Highly improved reverse osmosis performance of novel PVA/DGEBA cross-linked membranes by incorporation of Pluronic F-127 and MWCNTs for water desalination, Desalination. 397 (2016) 53–66.

767 doi:10.1016/J.DESAL.2016.06.019.
768 [72] H. Choi, M. Son, S. Yoon, E. Celik, S. Kang, H. Park, C.H. Park, H. Choi,
769 Alginate fouling reduction of functionalized carbon nanotube blended cellulose
770 acetate membrane in forward osmosis, Chemosphere. 136 (2015) 204–210.
771 doi:10.1016/J.CHEMOSPHERE.2015.05.003.
772 [73] J. Farahbakhsh, M. Delnavaz, V. Vatanpour, Investigation of raw and oxidized
773 multiwalled carbon nanotubes in fabrication of reverse osmosis polyamide
774 membranes for improvement in desalination and antifouling properties,
775 Desalination. 410 (2017) 1–9. doi:10.1016/J.DESAL.2017.01.031.
776 [74] S.-M. Xue, Z.-L. Xu, Y.-J. Tang, C.-H. Ji, Polypiperazine-amide Nanofiltration
777 Membrane Modified by Different Functionalized Multiwalled Carbon
778 Nanotubes (MWCNTs), ACS Appl. Mater. Interfaces. 8 (2016) 19135–19144.
779 doi:10.1021/acsami.6b05545.
780 [75] A. Khalid, A.A. Al-Juhani, O.C. Al-Hamouz, T. Laoui, Z. Khan, M.A. Atieh,
781 Preparation and properties of nanocomposite polysulfone/multi-walled carbon
782 nanotubes membranes for desalination, Desalination. 367 (2015) 134–144.
783 doi:10.1016/J.DESAL.2015.04.001.
784 [76] M. Kumar, M. Ulbricht, Low fouling negatively charged hybrid ultrafiltration
785 membranes for protein separation from sulfonated poly(arylene ether sulfone)
786 block copolymer and functionalized multiwalled carbon nanotubes, Sep. Purif.
787 Technol. 127 (2014) 181–191. doi:10.1016/J.SEPPUR.2014.03.003.
788 [77] J. Zheng, M. Li, K. Yu, J. Hu, X. Zhang, L. Wang, Sulfonated multiwall carbon

nanotubes assisted thin-film nanocomposite membrane with enhanced water flux and anti-fouling property, J. Memb. Sci. 524 (2017) 344–353. doi:10.1016/J.MEMSCI.2016.11.032.

[78] B. Kang, Y.-D. Li, J. Liang, X. Yan, J. Chen, W.-Z. Lang, Novel PVDF hollow fiber ultrafiltration membranes with antibacterial and antifouling properties by embedding N-halamine functionalized multi-walled carbon nanotubes (MWNTs), RSC Adv. 6 (2016) 1710–1721. doi:10.1039/C5RA24804C.

[79] H.J. Kim, Y. Baek, K. Choi, D.G. Kim, H. Kang, Y.S. Choi, J. Yoon, J.C. Lee, The improvement of antibiofouling properties of a reverse osmosis membrane by oxidized CNTs, RSC Adv. 4 (2014) 32802. doi:10.1039/C4RA06489E.

[80] E. Rusen, A. Mocanu, L.C. Nistor, A. Dinescu, I. Călinescu, G. Mustăţea, Ş.I. Voicu, C. Andronescu, A. Diacon, Design of Antimicrobial Membrane Based on Polymer Colloids/Multiwall Carbon Nanotubes Hybrid Material with Silver Nanoparticles, ACS Appl. Mater. Interfaces. 6 (2014) 17384–17393. doi:10.1021/am505024p.

[81] S. Wang, S. Liang, P. Liang, X. Zhang, J. Sun, S. Wu, X. Huang, In-situ combined dual-layer CNT/PVDF membrane for electrically-enhanced fouling resistance, J. Memb. Sci. 491 (2015) 37–44. doi:10.1016/J.MEMSCI.2015.05.014.

[82] Q. Zhang, C.D. Vecitis, Conductive CNT-PVDF membrane for capacitive organic fouling reduction, J. Memb. Sci. 459 (2014) 143–156. doi:10.1016/J.MEMSCI.2014.02.017.

[83] R. Hashaikeh, B.S. Lalia, V. Kochkodan, N. Hilal, A novel in situ membrane cleaning method using periodic electrolysis, J. Memb. Sci. 471 (2014) 149–154. doi:10.1016/J.MEMSCI.2014.08.017.

[84] X. Fan, H. Zhao, X. Quan, Y. Liu, S. Chen, Nanocarbon-based membrane filtration integrated with electric field driving for effective membrane fouling mitigation, Water Res. 88 (2016) 285–292. doi:10.1016/j.watres.2015.10.043.

[85] M.S. Rahaman, C.D. Vecitis, M. Elimelech, Electrochemical Carbon-Nanotube Filter Performance toward Virus Removal and Inactivation in the Presence of Natural Organic Matter, Environ. Sci. Technol. 46 (2012) 1556–1564. doi:10.1021/es203607d.

[86] X. Lu, X. Feng, X. Zhang, M.N. Chukwu, C.O. Osuji, M. Elimelech, Fabrication of a Desalination Membrane with Enhanced Microbial Resistance through Vertical Alignment of Graphene Oxide, Environ. Sci. Technol. Lett. 5 (2018) 614–620. doi:10.1021/acs.estlett.8b00364.

[87] H.-R. Chae, J. Lee, C.-H. Lee, I.-C. Kim, P.-K. Park, Graphene oxide-embedded thin-film composite reverse osmosis membrane with high flux, anti-biofouling, and chlorine resistance, J. Memb. Sci. 483 (2015) 128–135. doi:10.1016/J.MEMSCI.2015.02.045.

[88] J.-S. Lee, J.-C. Yoon, J.-H. Jang, A route towards superhydrophobic graphene surfaces: surface-treated reduced graphene oxide spheres, J. Mater. Chem. A. 1 (2013) 7312. doi:10.1039/c3ta11434a.

[89] J. Zhang, Z. Xu, M. Shan, B. Zhou, Y. Li, B. Li, J. Niu, X. Qian, Synergetic

effects of oxidized carbon nanotubes and graphene oxide on fouling control and anti-fouling mechanism of polyvinylidene fluoride ultrafiltration membranes, J. Memb. Sci. 448 (2013) 81–92. doi:10.1016/J.MEMSCI.2013.07.064.

[90] S.-Y. Yang, W.-N. Lin, Y.-L. Huang, H.-W. Tien, J.-Y. Wang, C.-C.M. Ma, S.-M. Li, Y.-S. Wang, Synergetic effects of graphene platelets and carbon nanotubes on the mechanical and thermal properties of epoxy composites, Carbon N. Y. 49 (2011) 793–803. doi:10.1016/J.CARBON.2010.10.014.

[91] J. Zhang, Z. Xu, W. Mai, C. Min, B. Zhou, M. Shan, Y. Li, C. Yang, Z. Wang, X. Qian, Improved hydrophilicity, permeability, antifouling and mechanical performance of PVDF composite ultrafiltration membranes tailored by oxidized low-dimensional carbon nanomaterials, J. Mater. Chem. A. 1 (2013) 3101. doi:10.1039/c2ta01415g.

[92] Y. Jiang, W.-N. Wang, D. Liu, Y. Nie, W. Li, J. Wu, F. Zhang, P. Biswas, J.D. Fortner, Engineered Crumpled Graphene Oxide Nanocomposite Membrane Assemblies for Advanced Water Treatment Processes, Environ. Sci. Technol. 49 (2015) 6846–6854. doi:10.1021/acs.est.5b00904.

[93] H.J. Kim, Y.-S. Choi, M.-Y. Lim, K.H. Jung, D.-G. Kim, J.-J. Kim, H. Kang, J.-C. Lee, Reverse osmosis nanocomposite membranes containing graphene oxides coated by tannic acid with chlorine-tolerant and antimicrobial properties, J. Memb. Sci. 514 (2016) 25–34. doi:10.1016/J.MEMSCI.2016.04.026.

[94] G. Ouyang, A. Hussain, J. Li, D. Li, Remarkable permeability enhancement of

855 polyethersulfone (PES) ultrafiltration membrane by blending cobalt
856 oxide/graphene oxide nanocomposites, RSC Adv. 5 (2015) 70448–70460.
857 doi:10.1039/C5RA11349K.
858 [95] M. Hu, S. Zheng, B. Mi, Organic Fouling of Graphene Oxide Membranes and
859 Its Implications for Membrane Fouling Control in Engineered Osmosis,
860 Environ. Sci. Technol. 50 (2016) 685–693. doi:10.1021/acs.est.5b03916.
861 [96] J.-L. Han, X. Xia, Y. Tao, H. Yun, Y.-N. Hou, C.-W. Zhao, Q. Luo, H.-Y.
862 Cheng, A.-J. Wang, Shielding membrane surface carboxyl groups by covalent-
863 binding graphene oxide to improve anti-fouling property and the simultaneous
864 promotion of flux, Water Res. 102 (2016) 619–628.
865 doi:10.1016/J.WATRES.2016.06.032.
866 [97] P.K.S. Mural, S. Jain, S. Kumar, G. Madras, S. Bose, Unimpeded permeation
867 of water through biocidal graphene oxide sheets anchored on to 3D porous
868 polyolefinic membranes, Nanoscale. 8 (2016) 8048–8057.
869 doi:10.1039/C6NR01356B.
870 [98] F. Perreault, H. Jaramillo, M. Xie, M. Ude, L.D. Nghiem, M. Elimelech,
871 Biofouling Mitigation in Forward Osmosis Using Graphene Oxide
872 Functionalized Thin-Film Composite Membranes, Environ. Sci. Technol. 50
873 (2016) 5840–5848. doi:10.1021/acs.est.5b06364.
874 [99] F. Perreault, M.E. Tousley, M. Elimelech, Thin-Film Composite Polyamide
875 Membranes Functionalized with Biocidal Graphene Oxide Nanosheets,
876 Environ. Sci. Technol. Lett. 1 (2014) 71–76. doi:10.1021/ez4001356.

877 [100] W. Choi, J. Choi, J. Bang, J.-H. Lee, Layer-by-Layer Assembly of Graphene
878 Oxide Nanosheets on Polyamide Membranes for Durable Reverse-Osmosis
879 Applications, ACS Appl. Mater. Interfaces. 5 (2013) 12510–12519.
880 doi:10.1021/am403790s.
881 [101] W. Miao, Z.-K. Li, X. Yan, Y.-J. Guo, W.-Z. Lang, Improved ultrafiltration
882 performance and chlorine resistance of PVDF hollow fiber membranes via
883 doping with sulfonated graphene oxide, Chem. Eng. J. 317 (2017) 901–912.
884 doi:10.1016/J.CEJ.2017.02.121.
885 [102] Z. Xu, T. Wu, J. Shi, K. Teng, W. Wang, M. Ma, J. Li, X. Qian, C. Li, J. Fan,
886 Photocatalytic antifouling PVDF ultrafiltration membranes based on synergy of
887 graphene oxide and TiO2 for water treatment, J. Memb. Sci. 520 (2016) 281–
888 293. doi:10.1016/J.MEMSCI.2016.07.060.
889 [103] Y. Jiang, D. Liu, M. Cho, S.S. Lee, F. Zhang, P. Biswas, J.D. Fortner, In Situ
890 Photocatalytic Synthesis of Ag Nanoparticles (nAg) by Crumpled Graphene
891 Oxide Composite Membranes for Filtration and Disinfection Applications,
892 Environ. Sci. Technol. 50 (2016) 2514–2521. doi:10.1021/acs.est.5b04584.
893 [104] S.-R. Chae, S. Wang, Z.D. Hendren, M.R. Wiesner, Y. Watanabe, C.K.
894 Gunsch, Effects of fullerene nanoparticles on Escherichia coli K12 respiratory
895 activity in aqueous suspension and potential use for membrane biofouling
896 control, J. Memb. Sci. 329 (2009) 68–74. doi:10.1016/J.MEMSCI.2008.12.023.
897 [105] Y. Orooji, M. Faghih, A. Razmjou, J. Hou, P. Moazzam, N. Emami, M.
898 Aghababaie, F. Nourisfa, V. Chen, W. Jin, Nanostructured mesoporous carbon

polyethersulfone composite ultrafiltration membrane with significantly low protein adsorption and bacterial adhesion, Carbon N. Y. 111 (2017) 689–704. doi:10.1016/J.CARBON.2016.10.055.

[106] Z. Zeng, D. Yu, Z. He, J. Liu, F.-X. Xiao, Y. Zhang, R. Wang, D. Bhattacharyya, T.T.Y. Tan, Graphene Oxide Quantum Dots Covalently Functionalized PVDF Membrane with Significantly-Enhanced Bactericidal and Antibiofouling Performances, Sci. Rep. 6 (2016) 20142. doi:10.1038/srep20142.

[107] L. Ballinas, C. Torras, V. Fierro, R. Garcia-Valls, Factors influencing activated carbon-polymeric composite membrane structure and performance, J. Phys. Chem. Solids. 65 (2004) 633–637. doi:10.1016/J.JPCS.2003.10.043.

[108] L.-L. Hwang, J.-C. Chen, M.-Y. Wey, The properties and filtration efficiency of activated carbon polymer composite membranes for the removal of humic acid, Desalination. 313 (2013) 166–175. doi:10.1016/J.DESAL.2012.12.019.

[109] A. Ghaffar, X. Zhu, B. Chen, Biochar composite membrane for high performance pollutant management: Fabrication, structural characteristics and synergistic mechanisms, Environ. Pollut. 233 (2018) 1013–1023. doi:10.1016/J.ENVPOL.2017.09.099.

[110] D. Cohen-Tanugi, J.C. Grossman, Water Desalination across Nanoporous Graphene, Nano Lett. 12 (2012) 3602–3608. doi:10.1021/nl3012853.

[111] S. Liu, T.H. Zeng, M. Hofmann, E. Burcombe, J. Wei, R. Jiang, J. Kong, Y. Chen, Antibacterial Activity of Graphite, Graphite Oxide, Graphene Oxide, and

Reduced Graphene Oxide: Membrane and Oxidative Stress, ACS Nano. 5 (2011) 6971–6980. doi:10.1021/nn202451x.

[112] F. Rashidi, N.S. Kevlich, S.A. Sinquefield, M.L. Shofner, S. Nair, Graphene Oxide Membranes in Extreme Operating Environments: Concentration of Kraft Black Liquor by Lignin Retention, ACS Sustain. Chem. Eng. 5 (2017) 1002–1009. doi:10.1021/acssuschemeng.6b02321.

[113] S. Xia, M. Ni, T. Zhu, Y. Zhao, N. Li, Ultrathin graphene oxide nanosheet membranes with various d -spacing assembled using the pressure-assisted filtration method for removing natural organic matter, Desalination. 371 (2015) 78–87. doi:10.1016/j.desal.2015.06.005.

[114] Z.-B. Zhang, J.-J. Wu, Y. Su, J. Zhou, Y. Gao, H.-Y. Yu, J.-S. Gu, Layer-by-layer assembly of graphene oxide on polypropylene macroporous membranes via click chemistry to improve antibacterial and antifouling performance, Appl. Surf. Sci. 332 (2015) 300–307. doi:10.1016/J.APSUSC.2015.01.193.

[115] E. Yang, C.-M. Kim, J. Song, H. Ki, M.-H. Ham, I.S. Kim, Enhanced desalination performance of forward osmosis membranes based on reduced graphene oxide laminates coated with hydrophilic polydopamine, Carbon N. Y. 117 (2017) 293–300. doi:10.1016/J.CARBON.2017.03.005.

[116] C.A. Amadei, A. Montessori, J.P. Kadow, S. Succi, C.D. Vecitis, Role of Oxygen Functionalities in Graphene Oxide Architectural Laminate Subnanometer Spacing and Water Transport, Environ. Sci. Technol. 51 (2017) 4280–4288. doi:10.1021/acs.est.6b05711.

[117] X. Song, R.S. Zambare, S. Qi, B.N. Sowrirajalu, A.P. James Selvaraj, C.Y. Tang, C. Gao, Charge-Gated Ion Transport through Polyelectrolyte Intercalated Amine Reduced Graphene Oxide Membranes, ACS Appl. Mater. Interfaces. 9 (2017) 41482–41495. doi:10.1021/acsami.7b13724.

[118] Y. Wu, B. Cao, Assessment of Bacterial Survival in the Presence of Nanomaterials: Is Colony Forming Unit Count Sufficient?, Environ. Eng. Sci. 32 (2015) 977–977. doi:10.1089/ees.2015.0329.

[119] W. Li, X. Liu, Y.-N. Wang, T.H. Chong, C.Y. Tang, A.G. Fane, Analyzing the Evolution of Membrane Fouling via a Novel Method Based on 3D Optical Coherence Tomography Imaging, Environ. Sci. Technol. 50 (2016) 6930–6939. doi:10.1021/acs.est.6b00418.

[120] M. Mukherjee, N. V. Menon, X. Liu, Y. Kang, B. Cao, Confocal Laser Scanning Microscopy-Compatible Microfluidic Membrane Flow Cell as a Nondestructive Tool for Studying Biofouling Dynamics on Forward Osmosis Membranes, Environ. Sci. Technol. Lett. 3 (2016) 303–309. doi:10.1021/acs.estlett.6b00218.

[121] F. Du, L. Qu, Z. Xia, L. Feng, L. Dai, Membranes of Vertically Aligned Superlong Carbon Nanotubes, Langmuir. 27 (2011) 8437–8443. doi:10.1021/la200995r.

[122] A. Aqel, K.M.M.A. El-Nour, R.A.A. Ammar, A. Al-Warthan, Carbon nanotubes, science and technology part (I) structure, synthesis and characterisation, Arab. J. Chem. 5 (2012) 1–23.

965 doi:10.1016/J.ARABJC.2010.08.022.
966 [123] B. Mi, Graphene Oxide Membranes for Ionic and Molecular Sieving, Science
967 (80-.). 343 (2014) 740–742. doi:10.1126/science.1250247.
968 [124] S. Tan, W. Zou, F. Jiang, S. Tan, Y. Liu, D. Yuan, Facile fabrication of copper-
969 supported ordered mesoporous carbon for antibacterial behavior, Mater. Lett.
970 64 (2010) 2163–2166. doi:10.1016/J.MATLET.2010.07.023.
971 [125] Y. Ahmad Nor, H. Zhang, S. Purwajanti, H. Song, A.K. Meka, Y. Wang, N.
972 Mitter, D. Mahony, C. Yu, Hollow mesoporous carbon nanocarriers for
973 vancomycin delivery: understanding the structure–release relationship for
974 prolonged antibacterial performance, J. Mater. Chem. B. 4 (2016) 7014–7021.
975 doi:10.1039/C6TB01778A.
976 [126] S.C. Smith, D.F. Rodrigues, Carbon-based nanomaterials for removal of
977 chemical and biological contaminants from water: A review of mechanisms
978 and applications, Carbon N. Y. 91 (2015) 122–143.
979 doi:10.1016/J.CARBON.2015.04.043.
980 [127] K. Yang, B. Xing, Adsorption of Organic Compounds by Carbon
981 Nanomaterials in Aqueous Phase: Polanyi Theory and Its Application, Chem.
982 Rev. 110 (2010) 5989–6008. doi:10.1021/cr100059s.
983 [128] Z. Wu, D. Zhao, Ordered mesoporous materials as adsorbents, Chem.
984 Commun. 47 (2011) 3332. doi:10.1039/c0cc04909c.
985 [129] C. Zhang, K. Wei, W. Zhang, Y. Bai, Y. Sun, J. Gu, Graphene Oxide Quantum
986 Dots Incorporated into a Thin Film Nanocomposite Membrane with High Flux

and Antifouling Properties for Low-Pressure Nanofiltration, ACS Appl. Mater. Interfaces. 9 (2017) 11082–11094. doi:10.1021/acsami.6b12826.

[130] E. Raymundo-Piñero, F. Leroux, F. Béguin, A High-Performance Carbon for Supercapacitors Obtained by Carbonization of a Seaweed Biopolymer, Adv. Mater. 18 (2006) 1877–1882. doi:10.1002/adma.200501905.

[131] R.S. Gabhi, D.W. Kirk, C.Q. Jia, Preliminary investigation of electrical conductivity of monolithic biochar, Carbon N. Y. 116 (2017) 435–442. doi:10.1016/J.CARBON.2017.01.069.

[132] J.E. Fischer, H. Dai, A. Thess, R. Lee, N.M. Hanjani, D.L. Dehaas, R.E. Smalley, Metallic resistivity in crystalline ropes of single-wall carbon nanotubes, Phys. Rev. B. 55 (1997) R4921–R4924. doi:10.1103/PhysRevB.55.R4921.

[133] H. Dai, E.W. Wong, C.M. Lieber, Probing Electrical Transport in Nanomaterials: Conductivity of Individual Carbon Nanotubes, Science (80-.). 272 (1996) 523–526. doi:DOI: 10.1126/science.272.5261.523.

[134] A.B. Fuertes, S. Alvarez, Graphitic mesoporous carbons synthesised through mesostructured silica templates, Carbon N. Y. 42 (2004) 3049–3055. doi:10.1016/J.CARBON.2004.06.020.

[135] H.A. Alhashimi, C.B. Aktas, Life cycle environmental and economic performance of biochar compared with activated carbon: A meta-analysis, Resour. Conserv. Recycl. 118 (2017) 13–26. doi:10.1016/J.RESCONREC.2016.11.016.

[136] W.C. Ng, S. You, R. Ling, K.Y.-H. Gin, Y. Dai, C.-H. Wang, Co-gasification of woody biomass and chicken manure: Syngas production, biochar reutilization, and cost-benefit analysis, Energy. 139 (2017) 732–742. doi:10.1016/J.ENERGY.2017.07.165.

[137] B.A. Belmonte, M.F.D. Benjamin, R.R. Tan, Bi-objective optimization of biochar-based carbon management networks, J. Clean. Prod. 188 (2018) 911–920. doi:10.1016/J.JCLEPRO.2018.04.023.

[138] B. Asadishad, S. Ghoshal, N. Tufenkji, Short-Term Inactivation Rates of Selected Gram-Positive and Gram-Negative Bacteria Attached to Metal Oxide Mineral Surfaces: Role of Solution and Surface Chemistry, Environ. Sci. Technol. 47 (2013) 5729–5737. doi:10.1021/es4003923.

[139] T.-Y. Liu, Y. Tong, Z.-H. Liu, H.-H. Lin, Y.-K. Lin, B. Van der Bruggen, X.-L. Wang, Extracellular polymeric substances removal of dual-layer (PES/PVDF) hollow fiber UF membrane comprising multi-walled carbon nanotubes for preventing RO biofouling, Sep. Purif. Technol. 148 (2015) 57–67. doi:10.1016/J.SEPPUR.2015.05.004.

[140] J. Yin, G. Zhu, B. Deng, Multi-walled carbon nanotubes (MWNTs)/polysulfone (PSU) mixed matrix hollow fiber membranes for enhanced water treatment, J. Memb. Sci. 437 (2013) 237–248. doi:10.1016/J.MEMSCI.2013.03.021.

[141] H. Zhao, S. Qiu, L. Wu, L. Zhang, H. Chen, C. Gao, Improving the performance of polyamide reverse osmosis membrane by incorporation of

modified multi-walled carbon nanotubes, J. Memb. Sci. 450 (2014) 249–256. doi:10.1016/J.MEMSCI.2013.09.014.

[142] M. Kumar, M. Ulbricht, Novel antifouling positively charged hybrid ultrafiltration membranes for protein separation based on blends of carboxylated carbon nanotubes and aminated poly(arylene ether sulfone), J. Memb. Sci. 448 (2013) 62–73. doi:10.1016/J.MEMSCI.2013.07.055.

[143] V. Vatanpour, M. Esmaeili, M.H.D.A. Farahani, Fouling reduction and retention increment of polyethersulfone nanofiltration membranes embedded by amine-functionalized multi-walled carbon nanotubes, J. Memb. Sci. 466 (2014) 70–81. doi:10.1016/J.MEMSCI.2014.04.031.

[144] A. Rahimpour, M. Jahanshahi, S. Khalili, A. Mollahosseini, A. Zirepour, B. Rajaeian, Novel functionalized carbon nanotubes for improving the surface properties and performance of polyethersulfone (PES) membrane, Desalination. 286 (2012) 99–107. doi:10.1016/J.DESAL.2011.10.039.

[145] H. Zarrabi, M.E. Yekavalangi, V. Vatanpour, A. Shockravi, M. Safarpour, Improvement in desalination performance of thin film nanocomposite nanofiltration membrane using amine-functionalized multiwalled carbon nanotube, Desalination. 394 (2016) 83–90. doi:10.1016/J.DESAL.2016.05.002.

[146] J. Lee, Y. Ye, A.J. Ward, C. Zhou, V. Chen, A.I. Minett, S. Lee, Z. Liu, S.-R. Chae, J. Shi, High flux and high selectivity carbon nanotube composite membranes for natural organic matter removal, Sep. Purif. Technol. 163 (2016) 109–119. doi:10.1016/j.seppur.2016.02.032.

[147] Ihsanullah, T. Laoui, A.M. Al-Amer, A.B. Khalil, A. Abbas, M. Khraisheh, M.A. Atieh, Novel anti-microbial membrane for desalination pretreatment: A silver nanoparticle-doped carbon nanotube membrane, Desalination. 376 (2015) 82–93. doi:10.1016/J.DESAL.2015.08.017.

[148] A. Zhu, H.K. Liu, F. Long, E. Su, A.M. Klibanov, Inactivation of Bacteria by Electric Current in the Presence of Carbon Nanotubes Embedded Within a Polymeric Membrane, Appl. Biochem. Biotechnol. 175 (2015) 666–676. doi:10.1007/s12010-014-1318-z.

[149] G.S. Ajmani, H.-H. Cho, T.E. Abbott Chalew, K.J. Schwab, J.G. Jacangelo, H. Huang, Static and dynamic removal of aquatic natural organic matter by carbon nanotubes, Water Res. 59 (2014) 262–270. doi:10.1016/j.watres.2014.04.030.

[150] L. Bai, H. Liang, J. Crittenden, F. Qu, A. Ding, J. Ma, X. Du, S. Guo, G. Li, Surface modification of UF membranes with functionalized MWCNTs to control membrane fouling by NOM fractions, J. Memb. Sci. 492 (2015) 400–411. doi:10.1016/J.MEMSCI.2015.06.006.

[151] A.K. Shukla, J. Alam, M. Alhoshan, L.A. Dass, M.R. Muthumareeswaran, Development of a nanocomposite ultrafiltration membrane based on polyphenylsulfone blended with graphene oxide, Sci. Rep. 7 (2017) 41976. doi:10.1038/srep41976.

[152] M.E.A. Ali, L. Wang, X. Wang, X. Feng, Thin film composite membranes embedded with graphene oxide for water desalination, Desalination. 386 (2016) 67–76. doi:10.1016/J.DESAL.2016.02.034.

[153] S. Zinadini, A.A. Zinatizadeh, M. Rahimi, V. Vatanpour, H. Zangeneh, Preparation of a novel antifouling mixed matrix PES membrane by embedding graphene oxide nanoplates, J. Memb. Sci. 453 (2014) 292–301. doi:10.1016/J.MEMSCI.2013.10.070.

[154] Z. Wang, H. Yu, J. Xia, F. Zhang, F. Li, Y. Xia, Y. Li, Novel GO-blended PVDF ultrafiltration membranes, Desalination. 299 (2012) 50–54. doi:10.1016/J.DESAL.2012.05.015.

[155] X. Chang, Z. Wang, S. Quan, Y. Xu, Z. Jiang, L. Shao, Exploring the synergetic effects of graphene oxide (GO) and polyvinylpyrrodione (PVP) on poly(vinylylidenefluoride) (PVDF) ultrafiltration membrane performance, Appl. Surf. Sci. 316 (2014) 537–548. doi:10.1016/J.APSUSC.2014.07.202.

[156] L. He, L.F. Dumée, C. Feng, L. Velleman, R. Reis, F. She, W. Gao, L. Kong, Promoted water transport across graphene oxide–poly(amide) thin film composite membranes and their antibacterial activity, Desalination. 365 (2015) 126–135. doi:10.1016/J.DESAL.2015.02.032.

[157] C. Zhao, X. Xu, J. Chen, G. Wang, F. Yang, Highly effective antifouling performance of PVDF/graphene oxide composite membrane in membrane bioreactor (MBR) system, Desalination. 340 (2014) 59–66. doi:10.1016/J.DESAL.2014.02.022.

[158] Z. Xu, J. Zhang, M. Shan, Y. Li, B. Li, J. Niu, B. Zhou, X. Qian, Organosilane-functionalized graphene oxide for enhanced antifouling and mechanical properties of polyvinylidene fluoride ultrafiltration membranes, J. Memb. Sci.

458 (2014) 1–13. doi:10.1016/J.MEMSCI.2014.01.050.

[159] R.S. Zambare, K.B. Dhopte, A. V. Patwardhan, P.R. Nemade, Polyamine functionalized graphene oxide polysulfone mixed matrix membranes with improved hydrophilicity and anti-fouling properties, Desalination. 403 (2017) 24–35. doi:10.1016/J.DESAL.2016.02.003.

[160] S. Aditya Kiran, Y. Lukka Thuyavan, G. Arthanareeswaran, T. Matsuura, A.F. Ismail, Impact of graphene oxide embedded polyethersulfone membranes for the effective treatment of distillery effluent, Chem. Eng. J. 286 (2016) 528–537. doi:10.1016/J.CEJ.2015.10.091.

[161] J. Zhu, M. Tian, J. Hou, J. Wang, J. Lin, Y. Zhang, J. Liu, B. Van der Bruggen, Surface zwitterionic functionalized graphene oxide for a novel loose nanofiltration membrane, J. Mater. Chem. A. 4 (2016) 1980–1990. doi:10.1039/C5TA08024J.

[162] J. Wang, Y. Wang, Y. Zhang, A. Uliana, J. Zhu, J. Liu, B. Van der Bruggen, Zeolitic Imidazolate Framework/Graphene Oxide Hybrid Nanosheets Functionalized Thin Film Nanocomposite Membrane for Enhanced Antimicrobial Performance, ACS Appl. Mater. Interfaces. 8 (2016) 25508–25519. doi:10.1021/acsami.6b06992.

[163] H. Wu, B. Tang, P. Wu, Development of novel SiO2–GO nanohybrid/polysulfone membrane with enhanced performance, J. Memb. Sci. 451 (2014) 94–102. doi:10.1016/J.MEMSCI.2013.09.018.

[164] Z.K. Li, W.Z. Lang, W. Miao, X. Yan, Y.J. Guo, Preparation and properties of

PVDF/SiO2@GO nanohybrid membranes via thermally induced phase separation method, J. Memb. Sci. 511 (2016) 151–161. doi:10.1016/J.MEMSCI.2016.03.048.

[165] Y.T. Chung, E. Mahmoudi, A.W. Mohammad, A. Benamor, D. Johnson, N. Hilal, Development of polysulfone-nanohybrid membranes using ZnO-GO composite for enhanced antifouling and antibacterial control, Desalination. 402 (2017) 123–132. doi:10.1016/J.DESAL.2016.09.030.

[166] M. Safarpour, V. Vatanpour, A. Khataee, Preparation and characterization of graphene oxide/TiO2 blended PES nanofiltration membrane with improved antifouling and separation performance, Desalination. 393 (2016) 65–78. doi:10.1016/J.DESAL.2015.07.003.

[167] M. Kumar, Z. Gholamvand, A. Morrissey, K. Nolan, M. Ulbricht, J. Lawler, Preparation and characterization of low fouling novel hybrid ultrafiltration membranes based on the blends of GO−TiO2 nanocomposite and polysulfone for humic acid removal, J. Memb. Sci. 506 (2016) 38–49. doi:10.1016/J.MEMSCI.2016.02.005.

[168] M. Safarpour, A. Khataee, V. Vatanpour, Thin film nanocomposite reverse osmosis membrane modified by reduced graphene oxide/TiO2 with improved desalination performance, J. Memb. Sci. 489 (2015) 43–54. doi:10.1016/J.MEMSCI.2015.04.010.

[169] H.M. Hegab, A. ElMekawy, T.G. Barclay, A. Michelmore, L. Zou, C.P. Saint, M. Ginic-Markovic, Effective in-situ chemical surface modification of forward

osmosis membranes with polydopamine-induced graphene oxide for biofouling mitigation, Desalination. 385 (2016) 126–137. doi:10.1016/J.DESAL.2016.02.021.

[170] H.M. Hegab, A. ElMekawy, T.G. Barclay, A. Michelmore, L. Zou, C.P. Saint, M. Ginic-Markovic, Single-Step Assembly of Multifunctional Poly(tannic acid)–Graphene Oxide Coating To Reduce Biofouling of Forward Osmosis Membranes, ACS Appl. Mater. Interfaces. 8 (2016) 17519–17528. doi:10.1021/acsami.6b03719.

[171] X. Huang, K.L. Marsh, B.T. McVerry, E.M. V. Hoek, R.B. Kaner, Low-Fouling Antibacterial Reverse Osmosis Membranes via Surface Grafting of Graphene Oxide, ACS Appl. Mater. Interfaces. 8 (2016) 14334–14338. doi:10.1021/acsami.6b05293.

[172] Y.L.F. Musico, C.M. Santos, M.L.P. Dalida, D.F. Rodrigues, Surface Modification of Membrane Filters Using Graphene and Graphene Oxide-Based Nanomaterials for Bacterial Inactivation and Removal, ACS Sustain. Chem. Eng. 2 (2014) 1559–1565. doi:10.1021/sc500044p.

[173] H.M. Hegab, Y. Wimalasiri, M. Ginic-Markovic, L. Zou, Improving the fouling resistance of brackish water membranes via surface modification with graphene oxide functionalized chitosan, Desalination. 365 (2015) 99–107. doi:10.1016/J.DESAL.2015.02.029.

[174] A.F. Faria, C. Liu, M. Xie, F. Perreault, L.D. Nghiem, J. Ma, M. Elimelech, Thin-film composite forward osmosis membranes functionalized with graphene

oxide–silver nanocomposites for biofouling control, J. Memb. Sci. 525 (2017) 146–156. doi:10.1016/J.MEMSCI.2016.10.040.

[175] N. Li, L. Liu, F. Yang, Highly conductive graphene/PANi-phytic acid modified cathodic filter membrane and its antifouling property in EMBR in neutral conditions, Desalination. 338 (2014) 10–16. doi:10.1016/J.DESAL.2014.01.019.

[176] F. Perreault, A. Fonseca de Faria, M. Elimelech, Environmental applications of graphene-based nanomaterials, Chem. Soc. Rev. 44 (2015) 5861–5896. doi:10.1039/C5CS00021A.

1173 Table 1. Material properties of CBMs used in antibiofouling membrane

	Activated carbon	Biochar	SWCNT	MWCNT	GO	Fullerene	Mesoporous carbon nanoparticle	Carbon quantum dot
Material feature	3D material	3D (nano)material	1D nanomaterial	1D nanomaterial	2D nanomaterial	0D nanomaterial	3D nanomaterial	0D nanomaterial
Water transport	NR[a]	NR	frictionless flow through CNT core (hydrophobic, smooth inner core)	frictionless flow through CNT core (higher water permeability then SWCNT) [121]	a) permeate through nanopore of GO sheet; b) permeate through interlayer space between adjacent GO nanosheets	No	NR	NR
Separation properties	NR	NR	Size exclusion (pore diameter: 0.6-100 nm) [122]	Size exclusion (pore diameter: 1-100 nm) [122]	Size exclusion: a) minimum pore size: 0.26 nm; b) 0.3-0.9 nm interspacing [123]	NR	NR	NR
Antibacterial	No	No	Physical damage, oxidative stress, metabolism disruption	Physical damage, oxidative stress, metabolism disruption (weaker than SWCNT)	Physical damage, ROS-dependent and ROS-independent oxidative stress	ROS production, metabolism disruption	No significant effects [105,124,125]	Physical damage, oxidative stress (GOQD[b]) (Zeng et al., 2012)
Adhesion affinity	High affinity to high molecular weight organics [126]	Similar with activated carbon	High affinity to various organic chemical [126]	High affinity to various organic chemical	Antiadhesion due to hydrophilicity and charge repulsion	Lower affinity and adsorption capability than CNT [127]	High affinity to various organic chemical [128]	Antiadhesion due to hydrophilic and charge repulsion (GOQD) [129]
Electrical conductivity (S/m)	30-80 [130]	10^{-6}-400 [131]	10^{6} [132]	10^{4}-10^{5} [133]	electrical insulation	10^{-6} – 10^{-12} (Mokarova et al., 2001)	30-500 [134]	Electrical insulation (GOQD)
Market Price ($/g)	0.3-2.1*10^{-3} [135]	0.1-4.0*10^{-3} [136,137]	25-280	0.6-25	125 -300	35-400	30-160	2000-7500

1174 [a]NR: no reference; [b]GOQD: graphene oxide quantum dot.

1175

1176 Table 2. Summary of the use of CNTs for membrane modification

Category[a]	Base polymer	Filtration process[b]	Carbon material[c]	Fabrication method	Pure water permeability (modified vs control)	Antibacterial effect	Antifouling effect[d]	Feed solution[e]	Reference
Vertically aligned	Epoxy	UF	SWCNT	Casting	231%	-	2 log less cell attachment	*P. aeruginosa* PAO1	[66]
	-	UF	SWCNT wall	Densification	2,466.7%	-	Qualitative	*P. aeruginosa* PA01	[68]
	PVDF	NF	MWCNT	Deposition	-		FRR 82%	BSA	[44]
	Polyamide	RO	SWCNT-Z	Interfacial polymerization	-	-	FRR increased by 44.9%, R_t decreased 28.2%	BSA	[67]
MM in active and support layer	PSF	NF and FO	CNT	Interfacial polymerization	143.4%	-	FRR increased by55.4% (NF), 15.6% (FO), R_t decreased by 39.8%(NF), 50%(FO)	HA	[138]
MM in support layer	PES	RO	MWCNT-COOH	Phase inversion	-	-	FRR increased by 6.64%, R_t increased by 6.48%	BSA	[70]
MM in active layer	Pluronic F-127 modified PVA	RO	MWCNT	Interfacial polymerization	-	80% growth inhibition	-	*E. coli*	[71]
	PES/PVDF	UF (HFM)	MWCNT-COOH	Phase inversion	463%	-	R_t decreased by 68.9%	BSA	[139]
	PSU	UF (HFM)	MWCNT-COOH	Phase inversion	196%	-	R_t decreased by 78.7%	BSA	[140]
	CA	FO	MWCNT-COOH	Phase inversion	-	-	R_t decreased by 23.5%	Alginate	[72]
	Polyamide	RO	MWCNT-COOH	Interfacial polymerization	-	-	FRR increased by 7%, R_t decreased by 10.8%	BSA	[141]
	PAES and APAES	UF	MWCNT-COOH	Phase inversion	150%	-	FRR increased by 17.7%, R_t decreased by 13.6%	Ovalbumin, lysozyme	[142]
	PVDF	RO	MWCNT-COOH	Interfacial polymerization	-	-	R_t decreased 58.9%	BSA	[73]
	PES	NF	MWCNT-NH_2	Phase inversion	174.3%	-	FRR increased by 46.1%	BSA	[143]
	PES	UF	MWCNT-NH_2	Phase inversion	148%	-	FRR increased by 70.4%, R_t decreased by 3.9%	BSA	[144]
	Polyamide	NF	MWCNT-NH_2	Interfacial polymerization	-	-	R_t decreased by 44.6%	BSA	[145]
	PAES/S-PAES	UF	MWCNT-SO_3H	Phase inversion	176%	-	FRR increased by 14.3%, R_t decreased by 24%	BSA	[142]
	PES	NF	MWCNT-SO_3H	Interfacial polymerization	160%	-	FRR increased by 11.2%, R_t decreased 40%	BSA	[77]
	PVDF	UF	MWCNT-HPAE	Phase inversion	485%	-	FRR increased by 22.1%, R_t increased by 6.2%	BSA	[41]

	PSF	NF	MWCNT-DDA	Phase inversion	275%	-	FRR increased by 45.6%, R_t decreased by 43.1%	BSA	[75]
	PVDF	UF (HFM)	MWCNT-CDDAC	Phase inversion	211%	Sterilization ratio 92.7% (*E. coli*) and 95.2% (*S. aureus*)	FRR increased by 52.4% (BSA)	BSA, *E. coli,* and *S. aureus*	[78]
	PES	UF	MWCNT-PANI	Phase inversion	564.5%	-	FRR 100%, R_t 65%	HA	[146]
	-	MF	MWCNT-AgNP	Sintering	-	100% removed/killed	-	*E. coli* K12	[147]
	PVDF	Charged UF	CNT	Phase inversion	-	-	R_t decreased by 85.8%	SRFA	[82]
	PSF	Charged MF	MWCNT-COOH	Phase inversion	-	Inactivated 99.999%	-	*E. coli*, *S. aureus*	[148]
Surface modification	PVDF	MF	SWCNT, MWCNT	Deposition	-	-	TMP decreased by 7.03 bar	Prefiltered natural surface water	[149]
	PVDF	Charged MF	MWCNT	Phase inversion	110%	-	TMP decreased by 14.8%	SA, BSA, HA mixture	[81]
	PES	UF	MWCNT-PEG	Deposition	98%	-	R_t decreased by 60% (HA); 41.8% (BSA); 9.4% (SA)	HA, BSA, and SA solution	[150]
	PSF	RO	MWCNT-COOH	Deposition	-	Cell viability less than 1%	R_t decreased by 67%	*P. aeruginosa* PAO1	[79]
	PAN	UF (HFM)	MWCNT-AgNP	Deposition	96%	86.7% growth inhibition	R_t decreased by 98%,FRR 91.8%	*E. coli*	[50]
	Styrene, acrylic acid	MF	MWCNT-AgNP	Deposition	-	Inhibition zone diameter increased by 3.67 mm (*S. aureus*) and 2.53 mm (*E. coli*)	-	*S. aureus* and *E. coli*	[80]

	PAN	Charged MF	CNT-COOH	Deposition	-	-	FRR 98%, R_t 15%	HA	[56]
	Polyamine	Charged UF	MWCNT-COOH	Interfacial polymerization	-	-	FRR 92.9%	BSA	[55]
	PVDF	Charged MF	MWCNT	Deposition	-	-	R_t 56.6%	Yeast	[83]
	Polyamide	Charged NF	MWCNT-COOH	Interfacial polymerization	667%	-	FRR 100%; flux decline rate three times lower than control	*P. aeruginosa* PA01	[52]
	PTFE	Charged MF	MWCNT	Deposition	-	7.4 log removal, 3.4 log inactivation	No fouling when filtering NOM	MS2 bacteriophage	[85]
	Ceramic	Charged MF (HFM)	CNT-COOH	Deposition	-	Qualitative	R_t 12.1%	*E. coli*	[84]

[a] MM: mixed matrix.

[b] UF: ultrafiltration; RO: reverse osmosis; MF: microfiltration; FO: forward osmosis; HFM: hollow fiber membrane.

[c] PANI: polyaniline; PEG: polyethlene glycol; Z: zwitterionic group; HPAE: hyperbranched poly(amine-ester); DDA: dodecylamine; CDDAC: (3-chloro-2-hydroxypropyl)-(5,5-dimethylhydantoinyl-1-ylmethyl)-dimethylammonium chloride.

[d] FRR: flux recovery rate; R_t: degree of the total flux loss caused by total fouling.

[e] SRFA: Suwannee river fulvic acid.

1184 Table 3. Summary of the application of graphene for membrane modification

Category	Base polymer[a]	Filtration process	Carbon material[b]	Fabrication method	Pure water permeability (modified vs control)	Antibacterial effect	Antifouling effect	Feed	Reference
MM in active and support layer	PSF	RO	GO	Interfacial polymerization	-	-	Biovolumes decreased by 99%	*P. aeruginosa* PAO1	[37]
MM in active layer	PPSU	UF	GO	Phase inversion	143.7%	-	R_t decreased by 58.3%, FRR increased by 72.7%	BSA	[151]
	PSF	UF	GO	Interfacial polymerization	-	-	R_t decreased by 44.2%, FRR increased by 70%	BSA	[152]
	PES	NF	GO	Phase inversion	248.8%	-	R_t decreased by 31.6%, FRR increased by 158.6%	Protein	[153]
	PVDF	UF	GO, OMWCNTs	Phase inversion	351.7%	-	R_t decreased by 6.1%, FRR increased by 554%	BSA	[89]
	PVDF	UF	GO, OMWCNTs	Phase inversion	340%	-	R_t decreased by 9.2%, FRR increased by 177.7%	BSA	[89]
	PVDF	UF	GO	Phase inversion	196.4%	-	FRR increased by 23%	BSA	[154]
	PVDF	UF	GO	Phase inversion	321.8%	-	FRR increased by 26.6%	BSA	[155]
	PA	FO	GO	Interfacial polymerization	163.9%	-	FRR increased by 60%	SA	[38]
	PA	UF	GO	Interfacial polymerization	180%	78.4% inactivation	-	*E. coli*	[156]

PA	RO	GO	Interfacial polymerization	-	-	Biovolume decreased by 98%	*P. aeruginosa* PA01	[87]
PSF	UF	GO	Phase inversion	151.4%	-	Biofilm thickness decreased by 43%	*P. aeruginosa* PAO1	[46]
PVDF	MF	GO	Phase inversion	151.5%	-	R_t decreased by 22%	Wastewater	[157]
PA	UF	GO	Interfacial polymerization	124.3%	-	R_t decreased by 71%	Natural water	[113]
PVDF (HFM)	UF	GO-SO_3H	Phase inversion	198.4%	-	R_t decreased by 36.6%, FRR increased by 8.7% (after five cycles)	HA	[101]
PVDF	UF	GO-SO_3H	Phase inversion	255.2%	-	R_t decreased by 7.9%, FRR increased by 76.3%	BSA	[57]
PVDF	UF	GO-APTS	Phase inversion	170.8%	-	R_t decreased by 63%, FRR increased by 203%	BSA	[158]
PSF	UF	GO-EDA	Phase inversion	303%	-	R_t decreased by 60.9%, FRR increased by 812.9%	BSA	[159]
PES	UF	GO–PAA	Phase inversion	244.1%	-	R_t decreased by 39.5% and 59.1%	Spent wash effluent	[160]
PES	NF	GO-PSBMA	Phase inversion	185.8%	-	R_t decreased by 68.6%, FRR increased by 68.8%	BSA	[161]
PA	RO	GO-TA	Interfacial polymerization	-	Viability decreased by 47.9%	-	*E. coli*	[93]
PES	NF	GO-ZIF8	Interfacial polymerization	152.6%	Inactivated 84.3%	-	*E. coli*	[162]

PSF	UF	GO-SiO_2	Phase inversion	182.2%	-	R_t increased by 5.8%, FRR increased by 16.1%	BSA	[163]
PVDF	UF	GO-SiO_2	Phase inversion	162.1%	-	R_t decreased by 37.3%, FRR increased by 23.2%	BSA	[35]
PVDF	UF	GO-SiO_2	Phase inversion	252.9%	-	R_t decreased by 28.9%, FRR increased by 103.6%	BSA	[164]
PSF	NF	GO-ZnO	Phase inversion	574.2%	Qualitative	R_t decreased by 9.2%, FRR increased by 16.5% (HA)	HA, *E. coli*	[165]
PES	NF	GO-TiO_2	Interfacial polymerization	100%	-	R_t decreased by 52.9%	BSA	[154]
PVDF	Photocatalytic UF	GO-TiO_2	Phase inversion	308.5%	-	R_t decreased by 52.1%, FRR increased by 90.5%	BSA	[102]
PES	NF	rGO-TiO_2	Phase inversion	194.8%	-	FRR increased by 28.7%	BSA	[166]
PSF	UF	GO-TiO_2	Phase inversion	104.5%	-	R_t decreased by 37.5%, FRR increased by 29.6%	HA	[167]
PES	Photocatalytic UF	GO−TiO_2-AgNP	Filtration	4.2%	3 log less live cells attached on membrane	-	*E.coli* K12	[92]
PA	RO	rGO-TiO_2	Interfacial polymerization	-	-	R_t decreased by 61.2%	BSA	[168]

	PES	UF	GO-Co_3O_4	Phase inversion	344.1%	Inactivated 89.8% (*E. coli*)	R_t decreased by 20.8%, FRR increased by 45.4% (activated sludge)	*E. coli*, activated sludge	[94]
	PVDF	UF	GO-AC	Phase inversion	88.3%	Biovolume decreased by 83.9%	R_t decreased by 2.8%, FRR increased by 1.8% (BSA)	*P. aeruginosa*, BSA	[36]
Surface modification	PA	RO	GO/GO-NH_2	Layer-by-layer assembly	-	-	R_t decreased by 55.9%	BSA	[100]
	PA	FO	GO-pDA	Covalent bonding	121.5%	ATP level decreased by 98.5%	R_t decreased by 37.1%	Surface water	[169]
	pDA/TMC	MF	GO	Layer-by-layer self-assembly	184.2%	-	R_t decreased by 47.2%	Alginate	[96]
	PA	PRO	GO	Layer-by-layer assembly	-	-	R_t decreased by 44.3%, FRR increased by 32.7%	Alginate	[95]
	PA	FO	GO	Covalent bonding	120%	ATP level decreased by 99.9%	R_t decreased by 18.5%, biofouling resistance increased by 33%	Surface water	[170]
	PA	FO	GO	Covalent bonding	-	Viability decreased by 32.6%, cell attachment decreased by 36%	R_t decreased by 50%	*P. aeruginosa*	[98]
	PE	MF	GO	Covalent bonding	-	99% bacterial inactivation	-	*E. coli*	[97]
	PA	RO	GO	Covalent bonding	96.7%	65% bacterial inactivation	-	*E. coli*	[99]
	PA	RO	GO-Azide	Covalent bonding	-	Cell adhesion reduced by 94.1%, 90% inactivated	R_t reduced by 42.9% (BSA)	*E. coli*, BSA solution	[171]

Polypropylene	UF	GO-alkynyl; GO-azide	Layer-by-layer assembly	182%	Viability decreased by 66.7%	R_t decreased by 26.1%, FRR increased by 86% (BSA)	*E. coli*, BSA	[114]
PA	FO	GO-PLL	Covalent bonding	105.9%	99% inactivation	R_t decreased by 21.7%	Surface water	[40]
Cellulose nitrate	UF	GO-PVK	Deposition	-	Viability reduced by 88.6% and 93.6%	-	*E. coli*, *B. subtilis*	[172]
PA	RO	GO-Cs	Covalent bonding	-	-	R_t decreased by 66.7%, FRR increased by 12.8%	BSA	[173]
PA	FO	GO-AgNP	Covalent bonding	-	Viability decreased by 80%, Live cell biovolume decreased by 41%	R_t decreased by 58.2%	*P. aeruginosa*	[174]
PES	UF	GO-TiO2-AgNP (*in situ*)	Covalent bonding	4.2%	3 log less live cells attached on membrane	-	*E. coli*, *B. subtilis*	[103]
PA	FO	GO-AgNP	Covalent bonding	98%	Viable cells decreased by 96%	-	*E. coli*	[39]
PANi, PA	Charged MF	rGO	Interfacial polymerization	15%	-	R_t decreased by 6.0%	Yeast	[175]
Polyester	Charged MF	rGO-PPy	Interfacial polymerization	-	-	R_t decreased by 5.2%	Yeast	[21]

[a] PA: polyamide; PPSU: polyphenylsulfone; PANi: polyaniline; pDA: polydopamine; TMC: 1,3,5-benzenetricarbonyl trichloride; PE: polyethylene.

[b] OMWCNTs: oxidized multiwall carbon nanotubes; TA: tannic acid; APTS: 3-aminopropyltriethoxysilane; EDA: ethylenediamine; PAA: polyacrylic acid; PSBMA: poly(sulfobetaine methacrylate); ZIF8: zeolitic imidazolate framework-8; Cs: chitosan; PLL: poly L-Lysine; PVK: poly(N-vinylcarbazole); PPy: polypyrrole; HNTs: halloysite nanotubes.

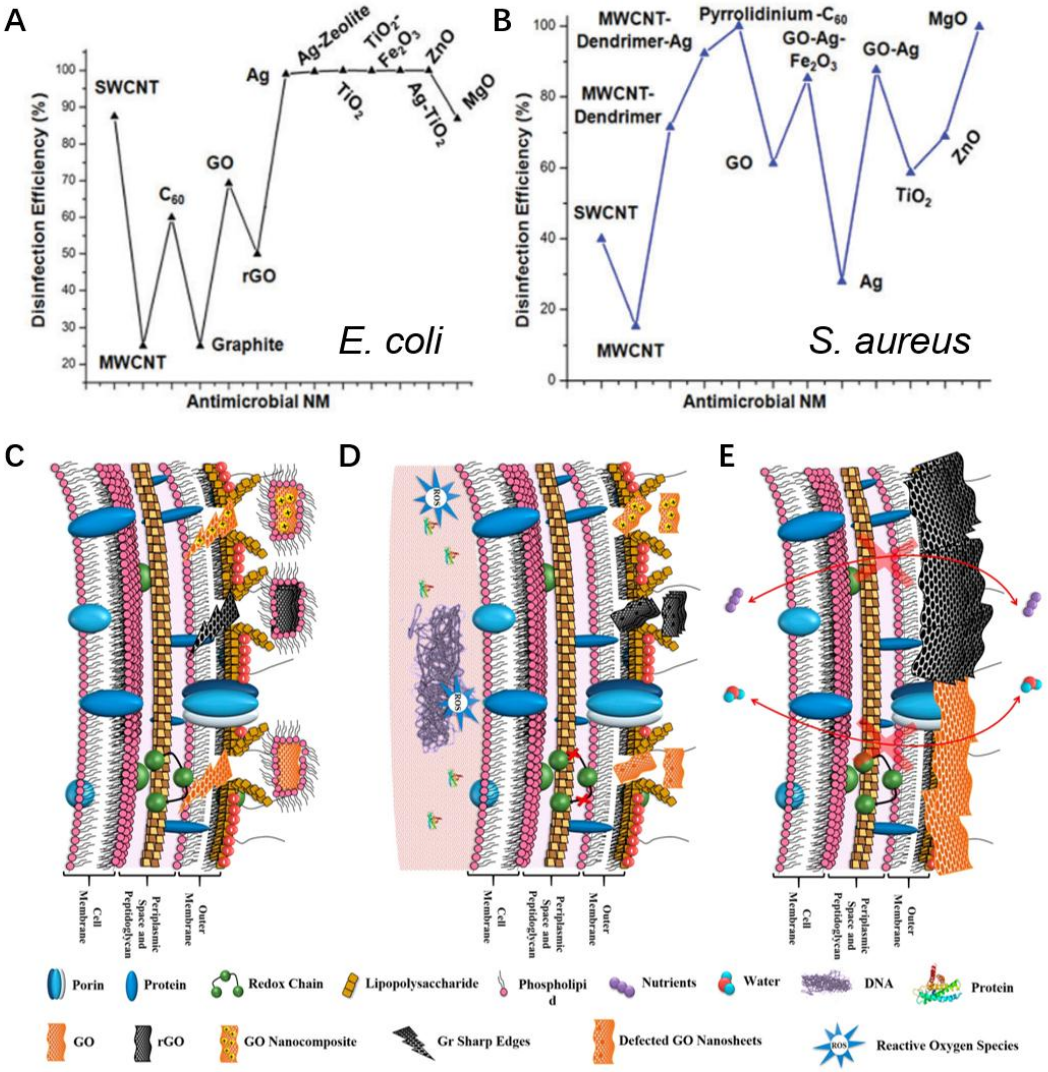

Figure 1. The disinfection efficiency of different nanomaterials and main antimicrobial mechanisms of graphene-family materials. GO, CNT and their derivatives displayed excellent antimicrobial activities against *E. coli* (A) and *S. aureus* (B). Direct physical damage (C); ROS-mediated oxidative stress (D); and bacterial isolation via wrapping around the bacterial surface (E). The figure is reprinted with copyright permission [27,29].

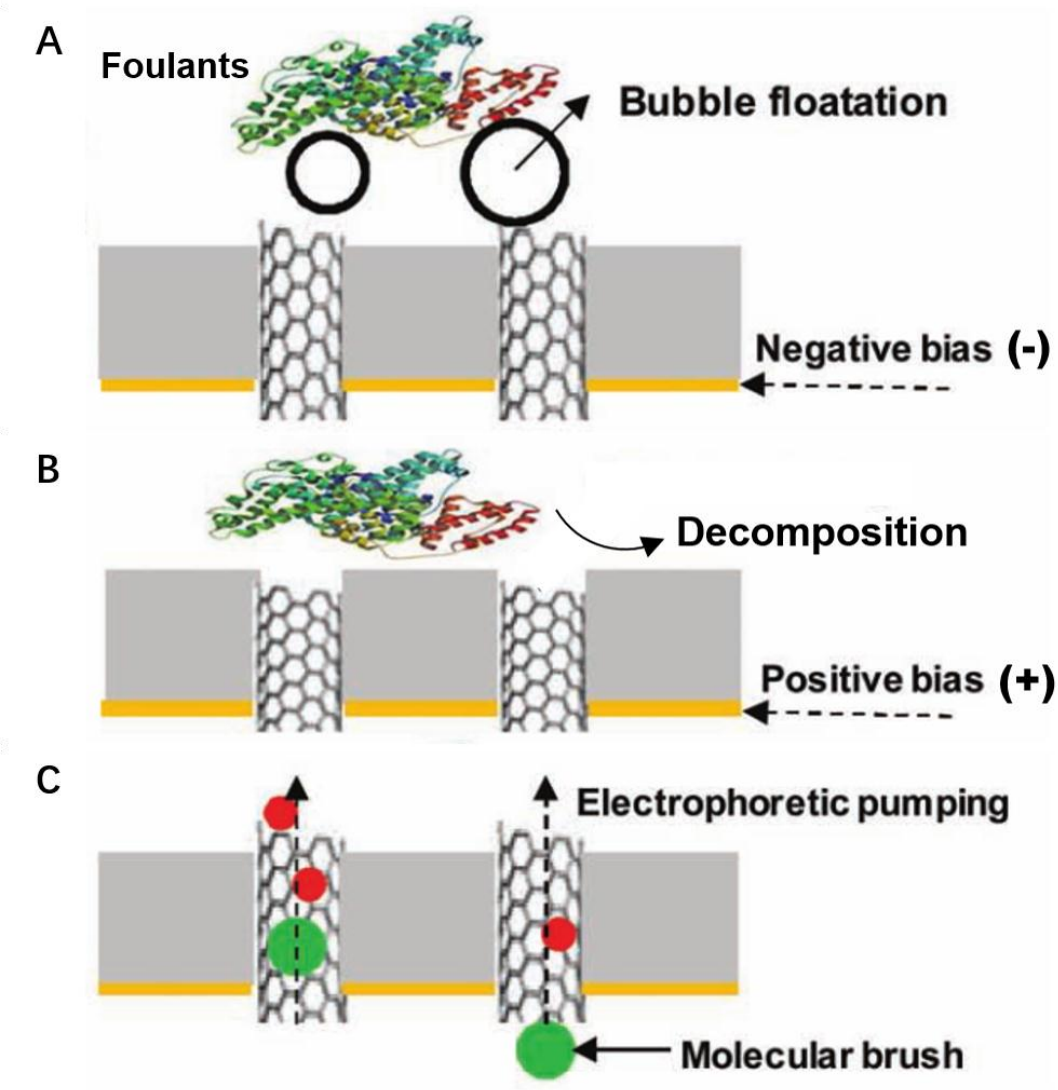

1199

1200 **Figure 2**. Schematic diagram of electrically-assisted fouling mitigation: membrane cleaning via
1201 bubbles generated by electro-reduction (A), foulants decomposed by electro-oxidation (B) and
1202 membrane cleaning via ionic pumping (C). The figures are reprinted with copyright permissions
1203 [2,54].

1204

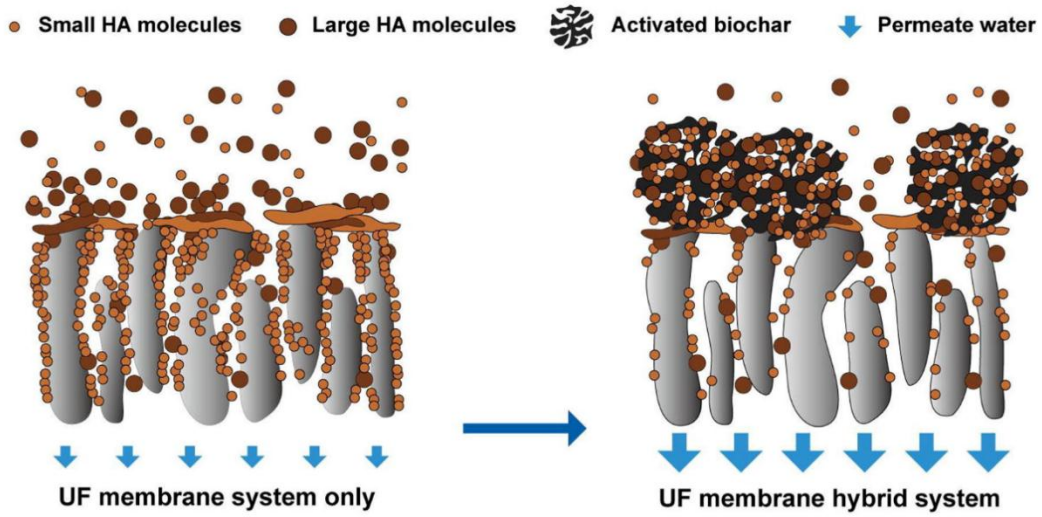

1205

1206 **Figure 3**. Application of biochar as an adsorbent to mitigate biofouling. The figure is reprinted with

1207 copyright permission [62].

1208

1209

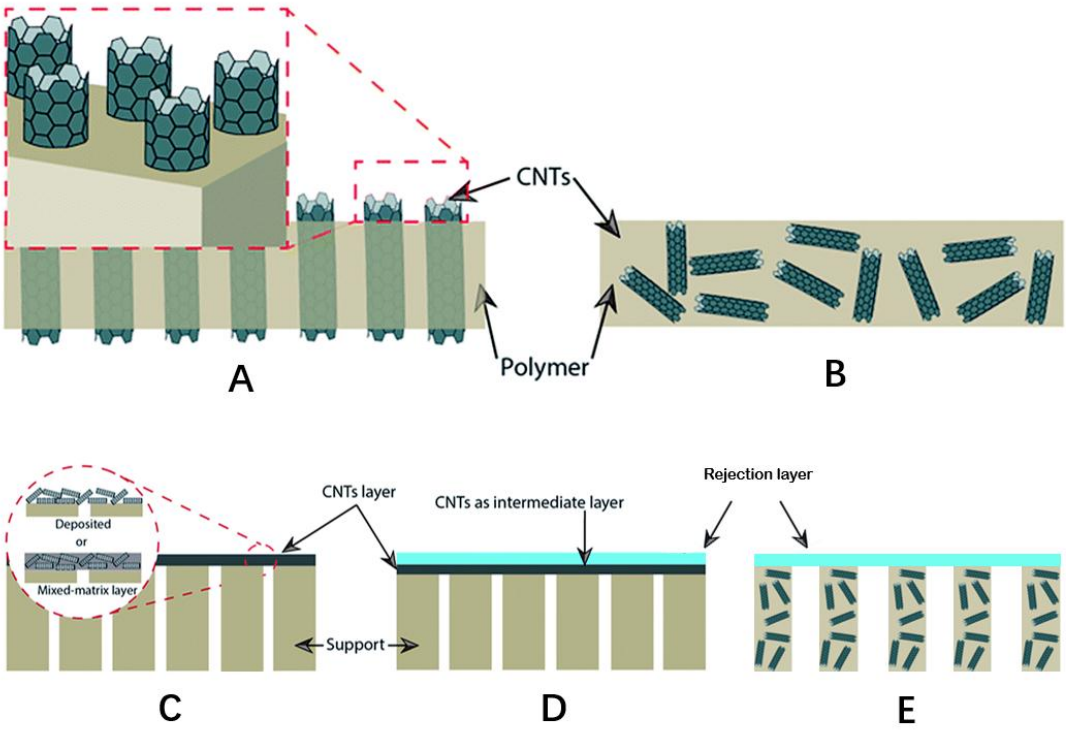

1210

1211 **Figure 4**. CNT membranes with different structures. Vertically aligned (A) and mixed matrix (B)

1212 CNT in membranes. CNT deposited on membrane surface or support (C). CNT coated on

1213 membrane surface (support) as intermediate layer (D). CNT incorporated in support layer (E) [32].

1214

1215

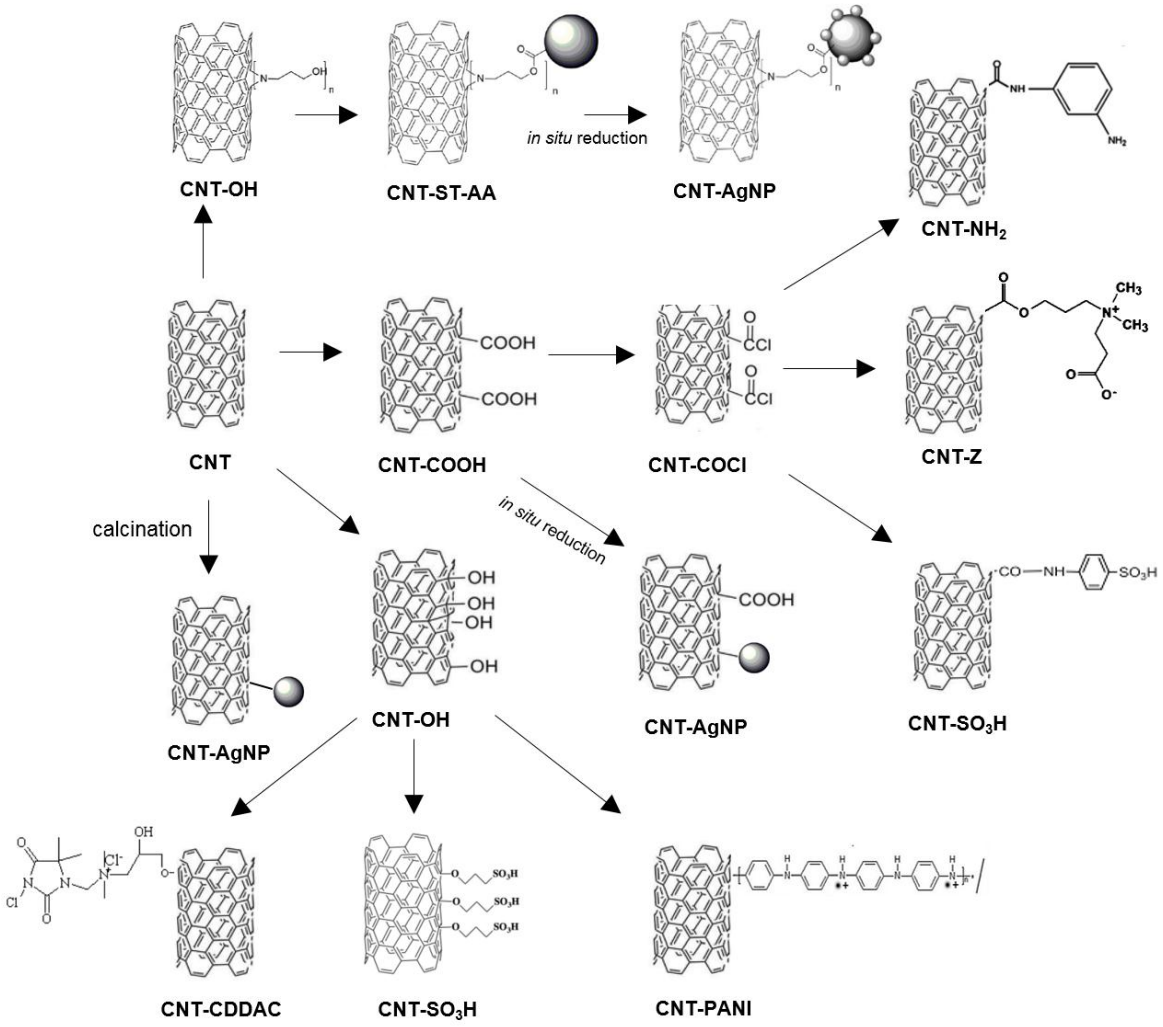

1216

1217 **Figure 5**. Functionalization of CNT for biofouling control. ST-AA: styrene-co-acrylic acid

1218 microspheres; Z: zwitterionic group; PANI: polyaniline; CDDAC: (3-chloro-2-hydroxypropyl)-

1219 (5,5-dimethylhydantoinyl-1-ylmethyl)-dimethylammonium chloride.

1220

1221

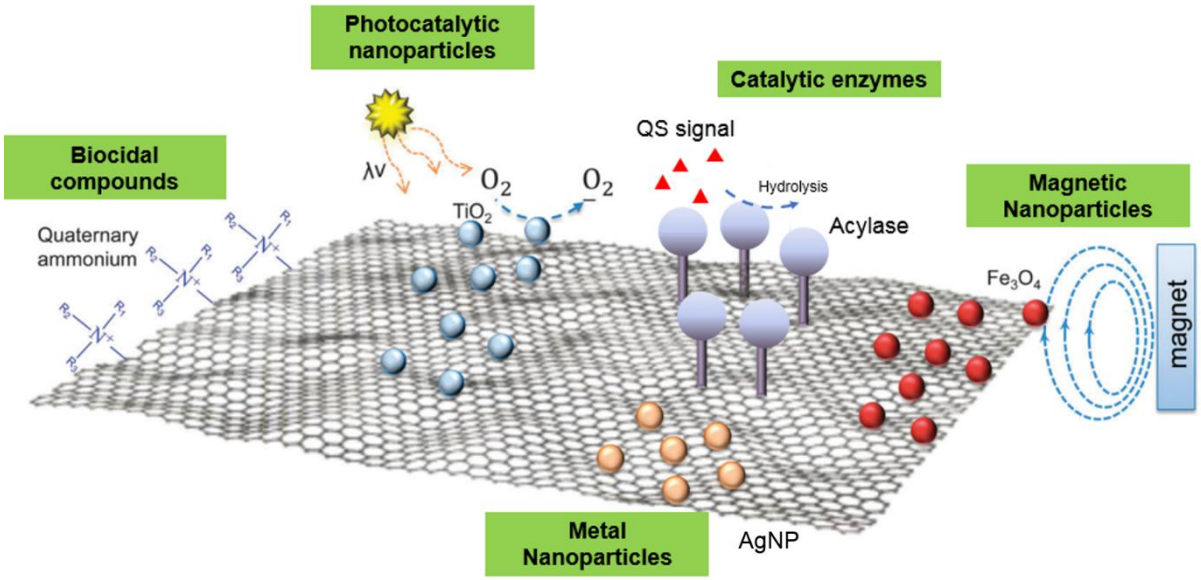

1222

1223 **Figure 6**. Different types of graphene-based antibiofouling nanocomposites [176].

1224